Hand Force Reflection using Pneumatic Muscle Actuators

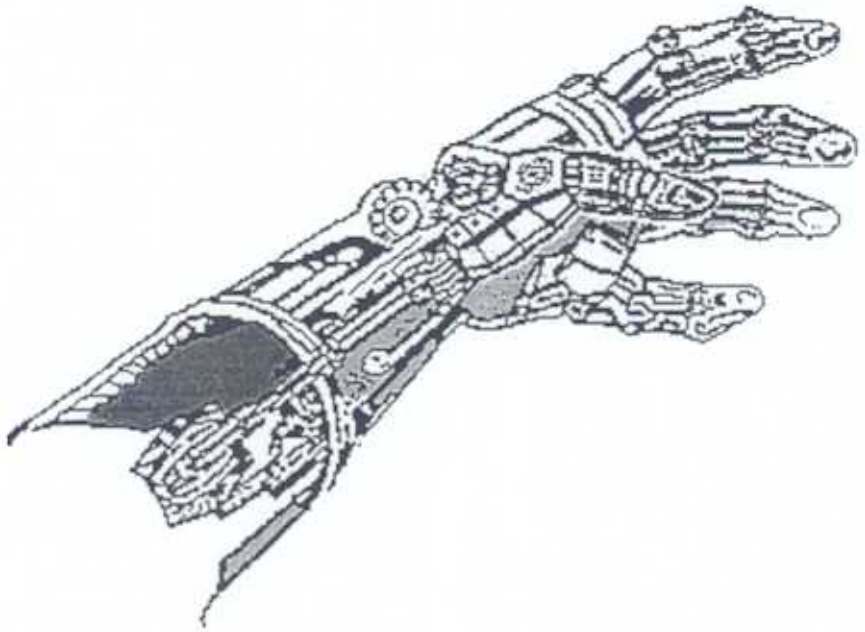

Quarterly Report

Contract F61708-98-W00134

Date 24-3-98

Report prepared by

C. Favede

Dept. of Electronic Eng.
University of Salford
Manchester, M5 4WT, UK

Report Documentation Page

Form Approved
OMB No. 0704-0188

1. REPORT DATE	2. REPORT TYPE	3. DATES COVERED
24 MAR 1998	**N/A**	**-**

4. TITLE AND SUBTITLE	5a. CONTRACT NUMBER
Hand Force Reflection using Pneumatic Muscle Actuators - Quarterly Report	5b. GRANT NUMBER
	5c. PROGRAM ELEMENT NUMBER
6. AUTHOR(S)	5d. PROJECT NUMBER
	5e. TASK NUMBER
	5f. WORK UNIT NUMBER
7. PERFORMING ORGANIZATION NAME(S) AND ADDRESS(ES) **University of Salford Manchester, M5 4WT, UK**	8. PERFORMING ORGANIZATION REPORT NUMBER
9. SPONSORING/MONITORING AGENCY NAME(S) AND ADDRESS(ES)	10. SPONSOR/MONITOR'S ACRONYM(S)
	11. SPONSOR/MONITOR'S REPORT NUMBER(S)

12. DISTRIBUTION/AVAILABILITY STATEMENT
Approved for public release, distribution unlimited

13. SUPPLEMENTARY NOTES
See also ADM001765 Hand Force Reflection Using Pneumatic Muscle Actuators.

14. ABSTRACT

15. SUBJECT TERMS

16. SECURITY CLASSIFICATION OF:			17. LIMITATION OF ABSTRACT	18. NUMBER OF PAGES	19a. NAME OF RESPONSIBLE PERSON
a. REPORT	b. ABSTRACT	c. THIS PAGE			
unclassified	**unclassified**	**unclassified**	**UU**	**77**	

Standard Form 298 (Rev. 8-98)
Prescribed by ANSI Std Z39-18

CONTENTS

Introduction - Progress update

Work on this project to develop a hand force reflection device using pneumatic muscles actuators has now been in progress for 3 months.
Progress to date has included:
i). an extensive study of the human hand and its skeletal and muscular behaviour,
ii). a comprehensive study of presently available force reflection hand masters,
iii). A study of the pneumatic muscle actuators and their models with a view to selection of muscles for use on the hand master,
iv). Specification of prototype 1 of the pneumatic muscle powered hand master,
v). Construction of muscles for the hand master.

These activities are discussed within this report. At this stage of the project, work is progressing in line with the plan outlined in the original proposal document. Based on the success to date, progress to the next stage will continue as planned. There is no need to change to work plan, and it is presently expected that progress towards the completion of stage 2 will be made on time and to budget.

1- THE HAND MOVEMENTS

The human hand, despite its complexity, turns out to be a perfectly logical structure, fully adapted to perform many actions, owing to its essential function : prehension. Prehension can also be performed by other animals such as the lobster with its pincers or the ape with its paws, but it reaches "perfection" only for the human hand. This is due to a special movement of the thumb (the movement of opposition) which brings it in contact with each finger [1].

The hand is the effector of the upper limb, which supports it mechanically and positions it in an optimal position for any given action. However, the hand is not only an effector but also a very accurate and sensitive receptor, which feeds back information such as texture, shape, weight and temperature, essential for its own performance. By itself, without the help of the eye, the hand is able to recognise an object.

For the purpose of this study, the hand will be divided into three parts : the palm, the fingers, and the thumb. The architecture of the hand is illustrated in Fig. 1.1.

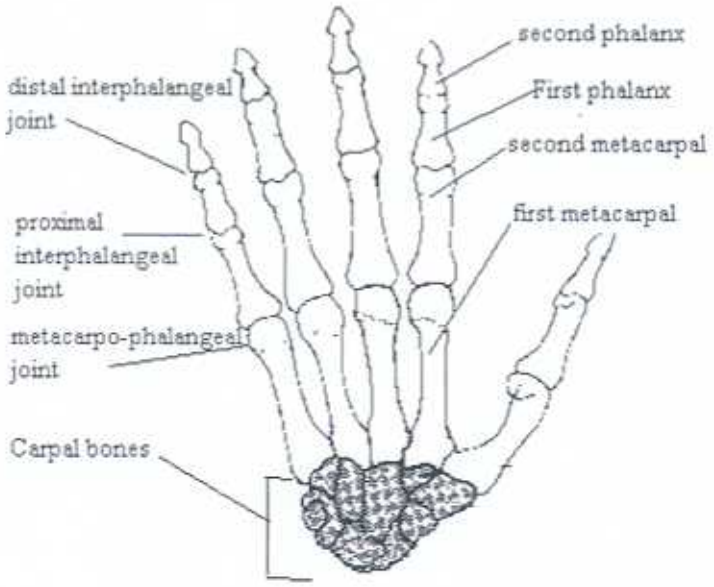

Fig. 1.1- The architecture of the human hand.

1.1- The palm.

The hollowing of the palm is due to two transverse arches :

i) The carpal arch : formed by the carpal bones of the wrist, this is concave in shape and allows a little movement

ii) The metacarpal arch : when the hand is flat the head of the last four metacarpal bones (the fifth metacarpal being ignored for the moment) lies in a straight line AB, as illustrated in Fig. 1.2.

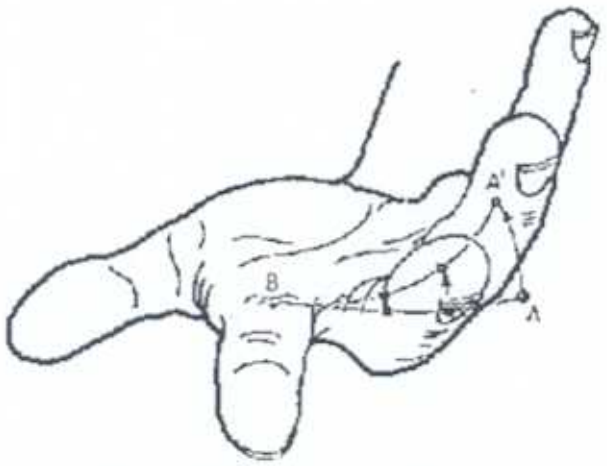

Fig. 1.2- The hollowing of the palm [1].

When the palm hollows, the head of the last three metacarpal bones move anteriorly, towards the palmar side of the hand, as shown in Fig. 1.3, and more so as the last finger is approached. Then the metacarpal heads lie on a curve A'B Fig. 1.2.
This capacity to widen and flatten provides much of the mobility of the palm of the hand.

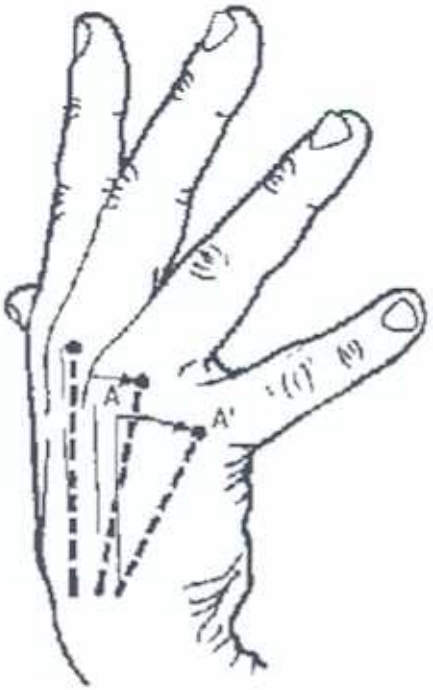

Fig. 1.3- Position of the metacarpal bones during the hollowing of the palm [1].

1.2- The fingers.

1.2.1- The metacarpo-phalangeal joints

These joints are of the condyloid type, with active movements around two axes at right angles and two degrees of freedom (DOF).

- Flexion and extension in a sagital plane, perpendicular to the surface of the palm.

- Adduction and abduction in a frontal plane, parallel to the surface of the palm.

These two movements greatly influence the function of the fingers. A passive rotation may also occur in association with the active movements, for example during gripping.

Active movement refers to the movement which a joint can do itself, whereas passive movement refers to the movement which a joint can do with an external help.

Flexion has a range of about 90° as illustrated in Fig. 1.4, it falls just short of 90° for the index but increases progressively with the other fingers.

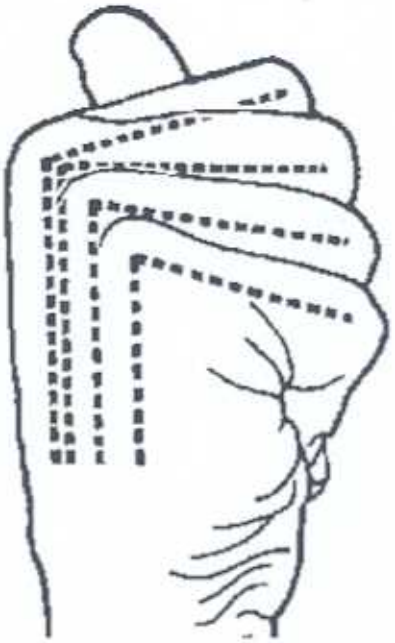

Fig. 1.4- Flexion of the metacarpo-phalangeal joint [1].

Active extension is variable and can reach up to 30° - 40°, passive extension can reach up to 90° (for people with very slack ligaments) [1].
Of all the fingers (with exception to the thumb) the index has the greatest range of abduction Fig. 1.5 (A) and adduction Fig.1.5 (B).

By a succession of simple movements, Fig. 1.6, of abduction (A), adduction (B), extension (C), and flexion (D), the index finger performs the movements of circumduction. This is defined by its base ABCD and its apex (metacarpo-phalangeal joint). This cone is flattened transversely because of the greater range of movement of flexion and extension. Its axis corresponds to the point of equilibrium of the metacarpo-phalangeal joint of the index.

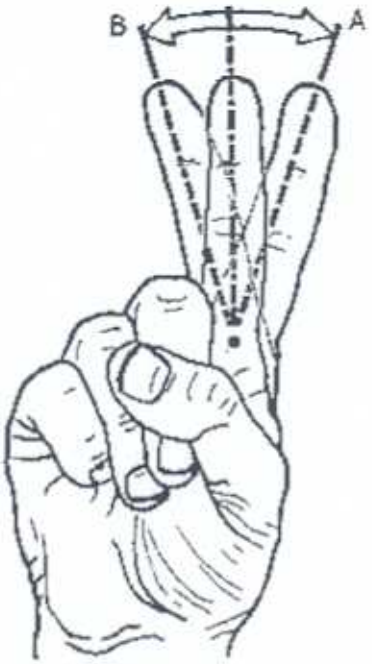

Fig. 1.5- Abduction and adduction of the finger [1].

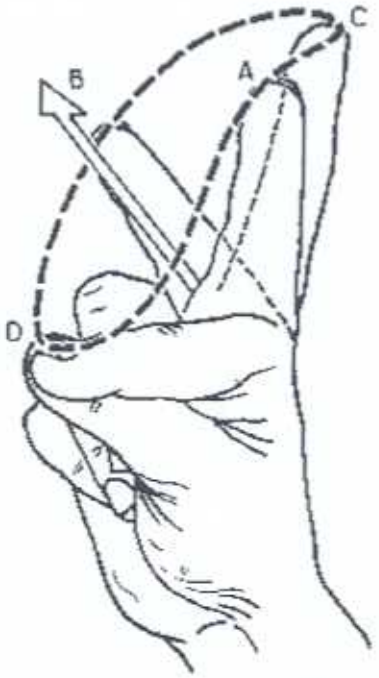

Fig. 1.6- Movement of circumduction [1].

1.2.2- The interphalangeal joints.

There are two interphalangeal joints per finger, the distal interphalangeal and the proximal interphalangeal joint. These joints are of the hinge type, with movement about one axis only and thus allow one DOF. This allows a movement of flexion and extension [3].

The range of flexion of the proximal interphalangeal joint is greater than 90°. As is the case for the metacarpo-phalangeal joint, flexion increases in range from the second to the fifth finger to reach a maximum of 135° for the latter, as illustrated in Fig. 1.7.

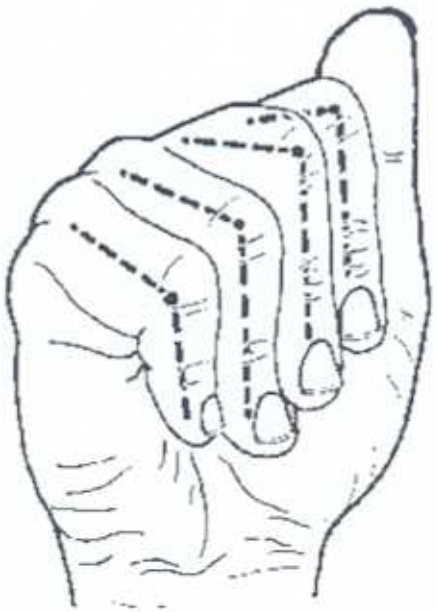

Fig. 1.7- Flexion of the proximal interphalangeal joint [1].

The range of flexion of the distal interphalangeal joints is slightly less than 90° as with the proximal interphalangeal joint [2]. This range increases from the second to the fifth to attain a maximum of 90° with the latter as shown in Fig. 1.8.

The range of active extension for both of the interphalangeal joints is 0°, and also for passive extension of the proximal interphalangeal joint, whereas for the distal interphalangeal joint passive extension can reach up to 30°.

Since the interphalangeal joints are of the hinge type there is no active but only a slightly passive abduction adduction movement especially at the distal interphalangeal joint.

Fig. 1.8- Flexion of the distal interphalangeal joint [1].

1.3- The thumb.

The thumb is the most important digit of the hand, as it is used in virtually all hand activities. It is essential in both power and precision grip (see section 1.4), because of its movement of opposition.

This pre-eminent role of the thumb is partly due to its location anterior to the palm and the other fingers. As shown in Fig. 1.9 this allows the thumb to move towards the fingers individually or collectively (the movement of opposition) and away from them (movement of counter-opposition).

The thumb consists of five bones lying along the lateral border of the hand as :

- the scaphoid (S)
- the trapezium (TZ)
- the first metacarpal (M1)
- the first phalanx (P1)
- the second phalanx (P2)

These five bones give four joints :

- The scapho-trapezium joint (ST) which gives only a very small movement of flexion and will not be considered in the latter part of this report.

- The trapezo-metacarpal joint (TM), which gives two DOF

- The metacarpo-phalangeal joint (MP), which allows two DOF

- The interphalangeal joint (IP), which allows one DOF

In sum, five DOF are needed to achieve the movement of opposition of the thumb.

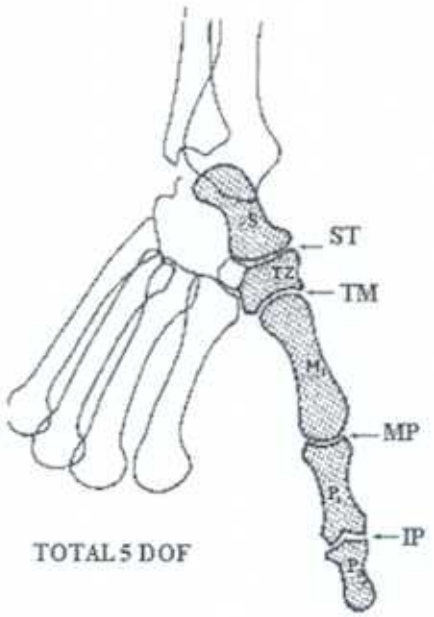

Fig. 1.9- Skeleton of the thumb [1].

1.3.1- The trapezo-metacarpal joint.

The trapezo-metacarpal joint plays an important role in the movement of the thumb, by allowing the thumb to take any position with respect to the hand. It is a saddle joint which allows the first metacarpal to move around two different axes and gives the movement of antepositiom and retroposition (see section 1.3.4) and the movement of flexion extension.

The range of retroposition is up to 15° - 25° while the range of anteposition is greater and reaches up to 25° - 35°. Flexion can reach up to 20° - 25° and extension is in the range of 30° to 45°.

1.3.2- The metacarpo-phalangeal joint.

The metacarpo-phalangeal joint is of the condyloid type, thus like the metacarpo-phalangeal joint of the fingers, it has two DOF allowing movements of flexion and extension and an abduction adduction movements. In fact, due to its complex architecture, it allows a third DOF allowing axial rotation of the first phalanx (pronation and supination).

The position of reference is when first phalanx and first metacarpal are collinear, from this position no active or passive extension is possible. Active flexion reaches 60° - 70°, as illustrated in Fig. 1.10, when passive flexion may reach up to 90°.

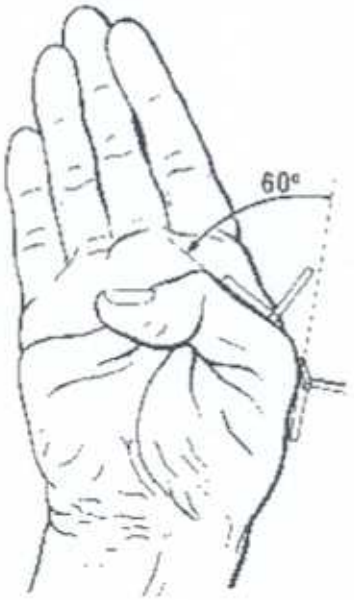

Fig. 1.10- Flexion of the metacarpo-phalangeal joint of the thumb [1].

The side to side movements and the pronation supination movements are controlled by the medial and lateral sesamoid muscles which can both contract when the thumb is in position of mid-flexion.

When the medial sesamoid muscle contracts, there is a medial displacement of a few degrees of the thumb and supination may reach 5° - 7°.

When the lateral sesamoid muscle contracts there is a lateral displacement which is greater than the medial displacement and a pronation of 20°.

1.3.3- The interphalangeal joint.

The interphalangeal joint of the thumb is a hinge joint which allows the movements of flexion and extension.

Active flexion can reach 75° - 80° while passive flexion is up to 90° as illustrated in Fig. 1.11.

Fig. 1.11- Flexion of the interphalangeal joint of the thumb [1].

Active extension is in the range of 5° - 10° but passive hyper extension can reach up to 30° as shown in Fig. 1.12.

1.3.4- Movements of opposition

Opposition is the essential movement of the thumb and brings the tip of the thumb into contact with that of any finger so as to form the pollicidigital pincer. Thus there is not only one movement of opposition but a series of movements of opposition, which shows a wide variety of static and dynamic grips depending on the shape of the object to be gripped and the number of fingers used for the grip.

The movement of opposition is a complex movement made by three components : anteposition, flexion and pronation.

Fig. 1.12- Extension of the interphalangeal joint of the thumb [1].

Anteposition is the movement that brings the thumb to lie anterior to the plane of the palm, as shown in Fig. 1.13. It takes place primarily at the trapezo-metacarpal joint and secondly at the metacarpo-phalangeal joint.

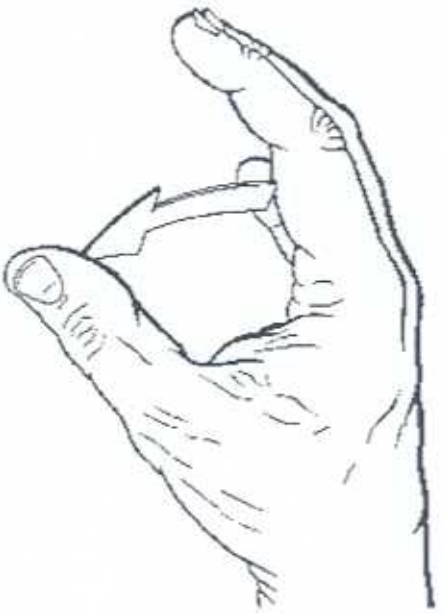

Fig. 1.13- Anteposition of the thumb [1].

Flexion moves the column of the thumb medially as illustrated in Fig. 1.14. All three joints of the thumb are involved, in particular the trapezo-metacarpal joint, but the metacarpo-phalangeal joint allows flexion of a variable degree as regards the finger chosen for opposition, and the interphalangeal joint supplements the metacarpo-phalangeal joint to achieve the movement.

Fig. 1.14- Flexion of the thumb [1].

Pronation (medial rotation) is essential, as it allows both pulps of the thumb and of the finger to achieve full contact as illustrated in Fig. 1.15. At its final position, in maximal opposition with the thumb touching the little finger, the movement of opposition is up to 90 -120°(Fig. 1.15).

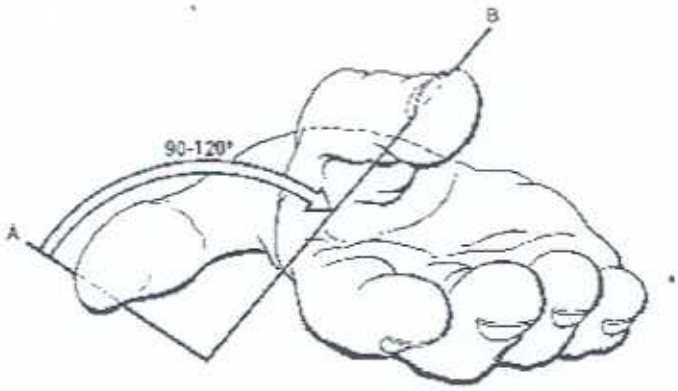

Fig. 1.15- Pronation of the thumb [1].

Opposition is essential during the grasping of any object, but in order to release the object, the thumb is able to achieve a movement of counter-opposition. This

movement possesses three components : retroposition, extension and supination (lateral rotation).

1-4. Grip.

The activity of the hand in daily life varies enormously. The five major functions of the hand are manipulation, sensation of touch, stabilisation (support), protection and communication. Manipulation is the most widely used. Prehensile movement can be classified into two main type :

- The power grip
- The precision or pinch grip

with several other less common types of grip such as the hook grip or the key grip [4].

Functionally, the hand can be divided into three components :

- the thumb, which by itself is involved in most of the functions of the hand because of its movement of opposition.
- the index and middle fingers which help the thumb to achieve precision grip.
- the ring and little finger which along with the rest of the hand are essential for grasping tool handles on the ulnar side of the hand and thus are vital for power grip [1].

Power grip is when an object is held in a clamp, formed by the partly flexed fingers and often a wide area of the palm, with counter pressure applied by the stable adducted thumb, as illustrated in Fig. 1.16.

The pinch grip or precision grip demands more exact control of the finger and the thumb position than in a power grip. The precision grip is carried out between the terminal opposing pulp part of the thumb and that of one or more of the fingers. With small objects the grip may involve the :

- the thumb and the index as illustrated in Fig. 1.17. (i)
- the thumb, the index and the middle finger as shown in Fig. 1.17 (ii)
- the thumb, the index, the middle and ring finger Fig. 1.17 (iii)

- the thumb and the four fingers as illustrated in Fig. 1.17 (iv)

Fig. 1.16 - Type of power grip [1].

Generally, the thumb is in a position of opposition. It is abducted and medially rotated at the carpometacarpal and metacarpo-phalangeal joints. It is held stable and forms one jaw of a clamp, with the opposing side formed in part or whole by the flexor surface of the terminal joint of the finger(s).

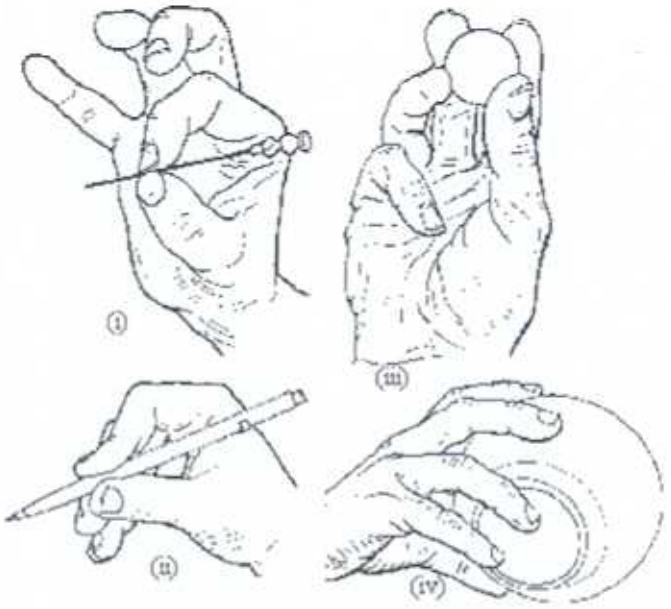

Fig. 1.17- Types of precision grip [1].

2-HAND MASTERS.

Hand masters are haptic interfaces that apply forces to the user's hand (and sometimes wrist) during the simulation of exploratory and manipulation tasks. Portable hand masters differ from the non-portable ones, because they are grounded on the user's forearm or palm. Therefore, the entire weight is sustained by the user remote from the body and may easily lead to user fatigue if the interface is heavy. Most of today's designs place actuators remote from the hand (either on the forearm, or on the user's back). From there, cables and pulleys transmit motion and torques to the hand. Another motivation for remote actuation is the small "area" available on the fingers and palm for placing these actuators. The more degrees of freedom that are active (up to 20 for the hand alone) the more actuators are needed, and more surface is required for them.

2.1- The University of Tsukuba Hand Master.

One of the first string-based portable hand masters for virtual haptic feedback was developed at the University of Tsukuba. To keep the structure light (only 0.25 kg) the device provides feedback to only two fingers (thumb and pointer) Fig. 2.1. This interface uses a string and pulley transmission to actuators placed on the dorsal side of the hand, permitting maximum freedom of motion for the fingers and allowing the grasping of real objects while the user is wearing the interface, because the palm area is free. A beam attachment on the back of the hand holds a rotary encoder that measures string displacement, a dc motor that provides up to 7-N feedback force, and a solenoid- actuated clutch. The clutch is used to simulate very hard objects by providing up to 20 N of resistive force at the fingertip. The controller driving the actuators has a bandwidth of 350 Hz. Simulation of grasping (and feeling) of virtual objects up to 9 cm in diameter is possible.

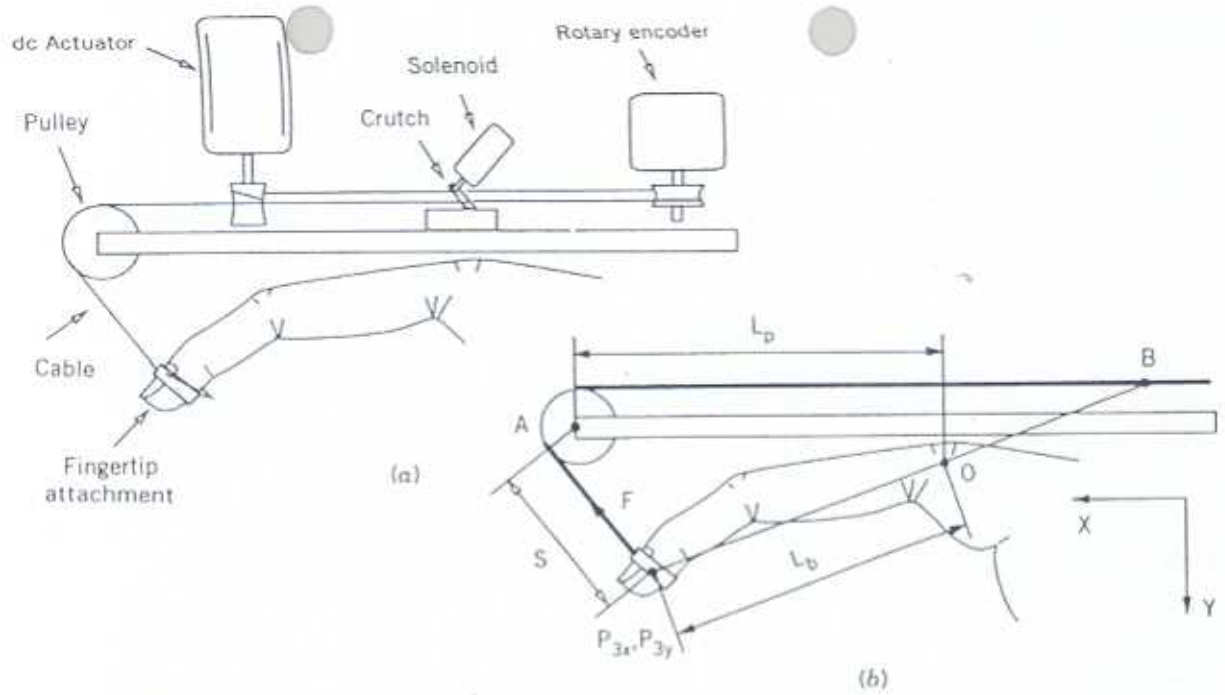

Fig. 2.1 - The University of Tsukuba Hand Master: (a) components; (b) geometry.[5]

2.2- The LRP Hand Master [5]

Another string-based hand master is the "LRP Hand Master" developed at the Laboratoire de Robotique de Paris (LRP). This haptic interface, Fig. 2.2, provides feedback to all fingers at 14 hand locations.

The LRP Hand Master places all the feedback structures on the back of the hand, leaving the palm free. This exoskeleton transmits forces from remote actuators using a combination of micro cables (0.45 mm in diameter), pulleys, and flexible links. The cable translation inside transmission sheaths is measured by potentiometers placed at the motor shafts. This data is then used to estimate hand configuration during the simulation.

The plastic-aluminium exoskeleton incorporates force sensors that measure cable strain, allowing for improved control despite cable friction and backlash. The feedback forces, which are normal to the finger segments during most of the grasping motion, are produced by dc disk motors. These actuators produce a continuous torque of 1.07 Nm and up to 11.48 Nm peak. All motors, power supply, and VME bus interface are placed in a separate control box.

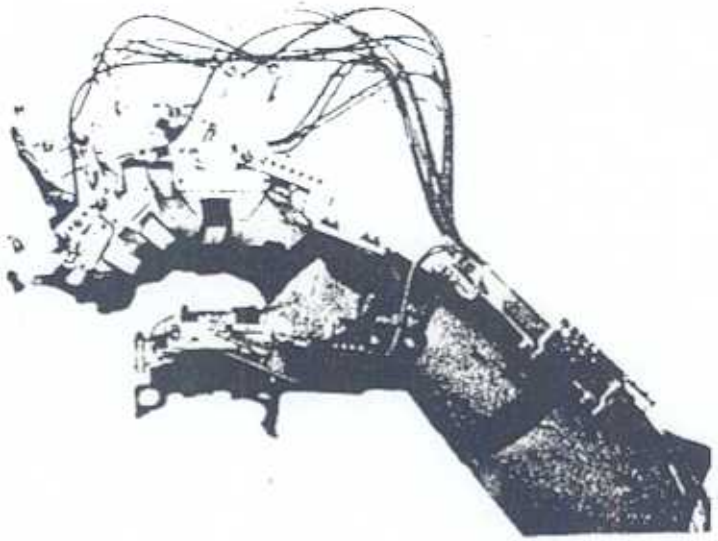

Fig. 2.2- The LRP Hand Master.

2.3- The ARTS Hand Force Feedback System [5].

The ARTS Hand Force Feedback System is a portable hand master which consists of a metacarpal plate and a glove-attached exoskeleton. The metacarpal plate has two degrees of freedom providing force feedback at the user's wrist. The plate functions as an attachment that allows the Hand Force Feedback System to connect to the distal end of the GLAD-IN-ART Arm Master [5]. The hand exoskeleton attaches to the back of the user's hand wearing a glove, as shown in Fig. 2.3. The exoskeleton mechanical attachments allow for the exertion of normal forces to each phalanx of the thumb, index, middle, and ring fingers. The palm area is left free, which allows for totally unencumbered motion (joint flexion of 80° to 90° and abduction/adduction of 150°. Position-sensing resolution for all degrees of freedom is very good (0.1°)

Feedback forces are exerted on each phalanx in the direction opposing grasping, up to a value of 1 N/phalanx. No force feedback is provided for abduction/adduction motion.

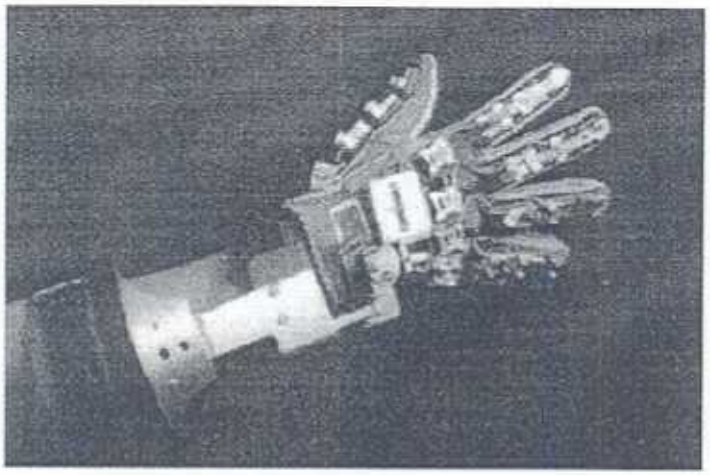

Fig. 2.3 - The GLAD IN ART.

2.4- The SAFIRE Master [5].

The SAFIRE was the first commercially available portable hand master. Similar to the ARTS hand master, the SAFIRE uses dc motors and cables to apply forces on the thumb, index, and middle fingers, Fig. 2.4. The actuators are placed on a structure on the back of the hand, thus leaving the palm area free. The master has two versions, namely SAFIRE 1 with five degrees of freedom and the SAFIRE II with eight degrees of freedom. Of these, the thumb and the index fingers have three degrees of freedom each, and the middle finger has two.

The SAFIRE allows a range of motion in flexion of 90°, whereas abduction/adduction and thumb anteposition is 45°. Each actuator has its own position encoder and torque sensor for improved force-feedback control.

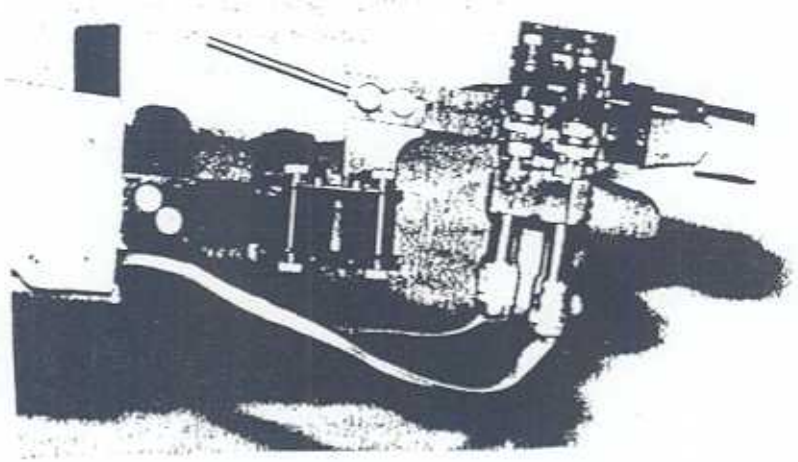

Fig. 2.4- The EXOS SAFIRE Hand Master.

The torques applied by the SAFIRE at the fingertips are 0.2 Nm. The total weight of the hand master is 1.5 kg for the SAFIRE II which raises concerns on user comfort for extended simulation time.

2.5- The Virtex CyberForce Glove [5] .

The previous hand masters have used metallic exoskeletons and cables to transmit forces and torques from remotely placed actuators. An alternative is the use of a double-layered glove with tendon attachments. By eliminating the metallic exoskeleton, the master is significantly lighter and therefore more comfortable to use. The drawbacks are increased friction and more difficult control from the compliance of the glove support.

A design of this type using a glove and Kevlar tendon, Fig. 2.5, which has not yet been patented. In addition to providing force feedback, this design also includes tactile feedback to the user's fingertips.

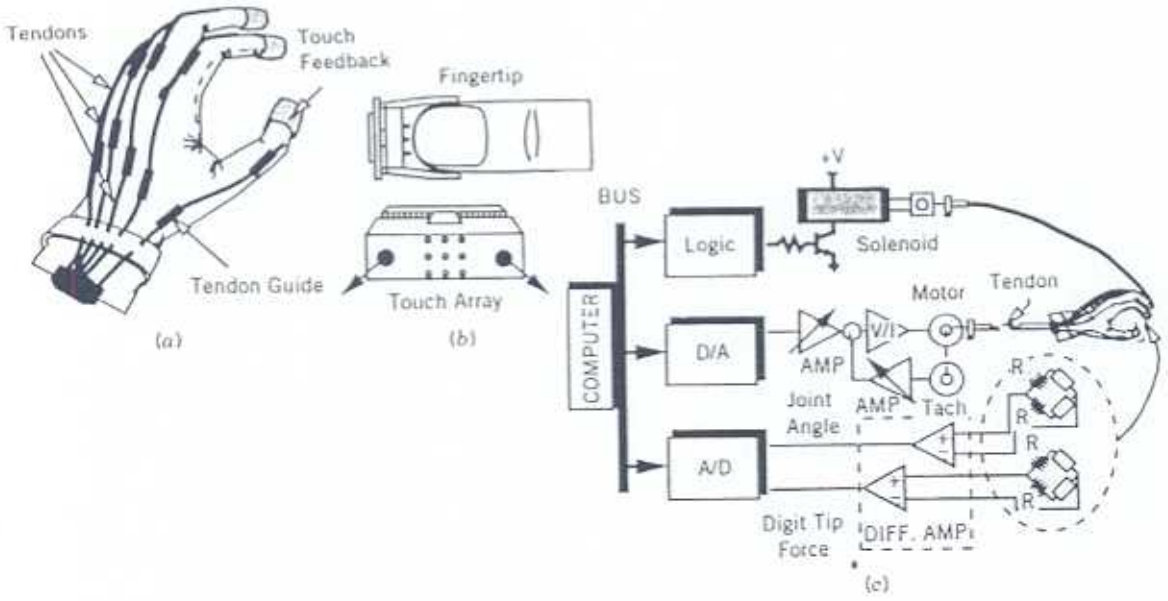

Fig. 2.5- The CyberForce Glove: (a) construction; (b) tactile array; (c) computer control.

Force feedback is produced by pushing the array metal support back against the finger. The tendons are actuated by dc motors under computer control through a D/A

board and power amplifiers. Hand position information, necessary to close the control loop is provided by position sensors integrated in the supporting glove

2.6- The CyberGrasp [6].

CyberGrasp is a 350 g force-reflecting exoskeleton that fits over a CyberGlove and adds resistive force feedback to each finger as illustrated in Fig. 2.6. The grasp forces are exerted via a network of tendons that are routed to the fingertips via an exoskeleton. The tendon sheaths are specifically designed for low compressibility and low friction. The actuators are high-quality DC motors located in a small enclosure on the desktop therefore the workspace of the CyberGrasp is limited to a one metre radius hemisphere. There are five actuators, one for each finger. The device exerts grasp forces that are roughly perpendicular to the fingertips throughout the range of motion, and forces can be specified individually, the maximum continuous force is 12 N. The CyberGrasp system allows full range-of-motion of the hand and does not obstruct the wearer's movements. The device is adjustable and designed to fit a variety of hands.

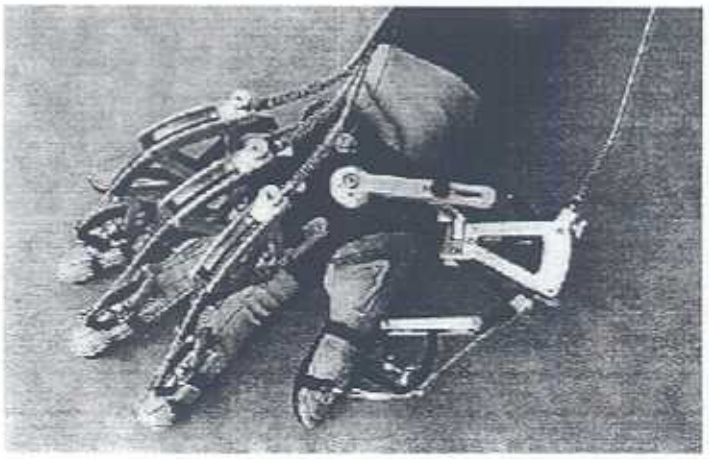

Fig. 2.6- The CyberGrasp.

2.7- The Rutgers Master I [5].

A direct-drive design that eliminates the need for cable transmission, by placing the actuators directly in the user's palm has been developed by Burdea at Rutgers University. This hand master called "Rutgers Master I" consists of four metallic microcylinders placed on a small L-shaped platform. The base of the pistons is coaxial with small spherical joints that allow the passage of small air tubes. Thus, each actuator has a conical work envelope that allows both finger flexion and adduction/abduction. The presence of the actuators in the palm does limit the hand mobility somewhat, with finger flexion of only 40° to 50° (depending on the particular finger joint). Abduction/adduction angles are not affected. As a safety measure the piston dimension is such that fingers cannot be pushed backward past their straight ("zero") posture. This fail-safe design prevents accidents in case of computer failure. Velcro attachments at the fingertip and the palm platform allow for adjustments for different user hand sizes.

The microcylinder actuators have a very good power-to-weight ratio, producing a force of 4 N at the fingertip (for air at 90 psi). The total weight of the feedback structure in the palm is less than 100 g, which is among the lightest of all hand masters. The actuator control is performed by proportional pressure regulators located in a separate control interface The force-feedback loop of the Rutgers Master I has a bandwidth of 11 to 14 Hz (depending on the type of proportional controller used) and closes asynchronously with the graphics loop.

2.7- The Rutgers Master II [5].

One of the difficulties with the Rutgers Master 1 was increased friction with actuator wear, up to 10% of the output. Another drawback was the hand master reliance on a commercial sensing glove for position sensing. This increased system costs and introduced unwanted sensing nonlinearities and coupling effects owing to the glove sensors. These problems were addressed in the design of the Rutgers Master II, Fig. 2.7.

The outward appearance of the Rutgers Master II is similar to the first model however all sensing has been integrated in the force-feedback structure, and the actuators were custom designed.

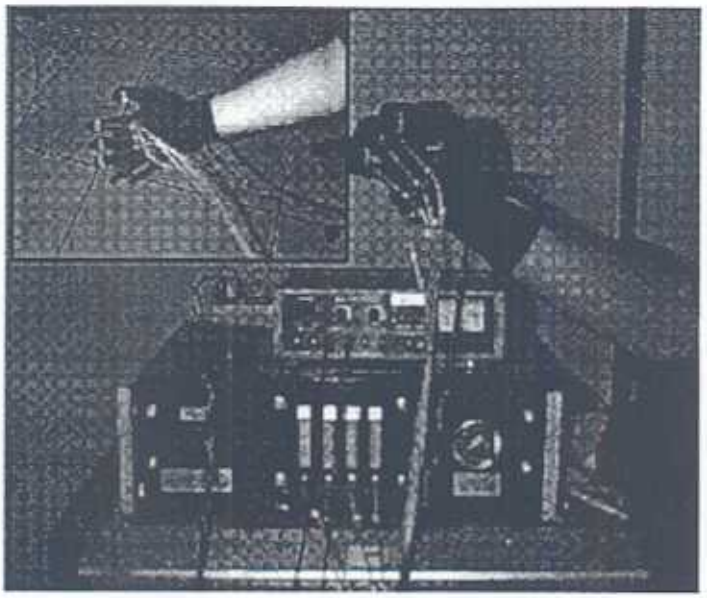

Fig. 2.5- The Rutgers Master II prototype.

When providing force feedback, it is important that sensing not introduce friction, therefore all the position sensors incorporated in the Rutgers Master II are noncontact. Each cylinder attaches to the palm platform through two revolute joints with Hall-effect position sensors. Thus, the fingertip position and orientation is sensed directly in Cartesian space and not in joint space, as done by other hand exoskeleton devices. Therefore position errors in each sensor are not additive, and the overall sensing accuracy increases. The actuator glass-graphite construction reduces friction, while the larger diameter increases the force feedback at the fingertip, producing fingertip forces up to 16.4 N (for 100 psi air pressure), four times more than the Rutgers Master I. Static friction in the cylinder accounts for only 0.05 N, which corresponds to a high dynamic range of 330.

The development of hand masters has made substantial progress in recent years. However, this study of the available technology has highlighted a number of

deficiencies in terms of complexity relatively to the human hand studies before and particularly in terms of the weight of the systems and the power to weight ratio of the actuators.

It is for this reason that the method of actuation will be addressed in this work, making use of a new range of pneumatic muscle actuators with excellent power to weight ratio and other helpful characteristics, will be studied subsequently.

3- PROJECT DEVELOPMENT

The pneumatic Muscle Actuators to be used in this work, figure 3.1, have been developed from activities in the early 1960's to produce a novel actuation system for artificial limb applications. Work at Salford has modified and improved these original designs tp provide a range of muscles with different characteristics and performance features. In addition models of the muscles have been produced to permit accurate controller design and these models have been used to provide force and position control of better than 1% of fsd [9].

Each muscle consists of an internal bladder surrounded by a braided mesh shell which are attached at either end to fittings or to some tendon-like structure. When the internal bladder is pressurised, the high pressure gas pushes against its inner surface and against the external shell, and tends to increase its volume. Due to the non extensibility of the threads in the braided mesh shell, the actuator shortens according to its volume increase and/or produces tension if it is coupled to a mechanical load. This physical configuration causes the muscles to have variable-stiffness spring-like characteristics, non-linear passive elasticity, physical flexibility, and is of a very light weight compare to other kind of actuators, which make it a good actuator to use for portable force feedback devices.

Fig. 3.1- The pneumatic muscle actuator.

3.1- Characteristics of the pneumatic muscle actuator.

The muscle can be pressurised between 1 bar to 8 bars (100-800kPa), producing a very powerful actuator with typically a power to weight ratio of about 400:1 This is significantly better than both pneumatic cylinders and DC motors that claim a ratio of only about 16:1 [9].

For the proposed hand force reflection system, each muscle will have a weight of approx. 20g which will give a total weight around 300g for the whole exoskeleton which is a much less than for the Safire master, and comparable with Tsukuba hand master but with force reflection on one more finger.

The muscles being proposed for use in the hand exoskeleton will be relatively small at 15cm in length with a diameter of 9mm but this muscle will have strength, speed and fine stroke control comparable with a finger muscle of a human hand.

In addition to its favourable strength and power/weight characteristics the pneumatic muscle is compliant, it can get wet, operate under water, be filled with liquid and even works when bent round a curved object. As with a pneumatic cylinder there is a linear stroke, but the friction is low and is completely constant, allowing proportional control with the possibility of very small step sizes. The muscle under pressure can produce a contraction up to 33% of its stretched length, accompanied by a force roughly inversely proportional to the degree of contraction. This property enables attachment of the muscle as close to the pivot point of a lever as wanted, and fine control over the mechanical advantage of the lever is possible [10].

The design of systems using the muscles becomes almost intuitive, because we can utilise almost any biological design. In this case the muscles will be mounted on the back of the hand as is the case for human muscles. This will give two further advantages in comparison to other designs:

i). As the muscles are not mounted in the palm area (cf Rutgers Hand I and II) the motion of the fingers during grasping will not be constraint by the actuators.

ii). The actuators will be directly grounded on the user hand, and not on a desk as for the CyberGrasp, therefore there will be no workspace limitation for this device.

3.2- Mathematics model and test of the pneumatic muscle [9,10].

The pneumatic air muscle is an actuator which converts pneumatic energy into mechanical energy by transferring the pressure applied on the inner surface of its bladder into the shortening tension. To find the relationship of the tension, length and pressure, a theoretical approach and several experiments will be analysed with simplified modelling.

In order to find the tension as a function of pressure and actuator length without considering the detailed geometric structure, a theoretical approach based on energy conservation is introduced.

The input work W_{in} is done in the pneumatic air muscle when gas pushes the inner bladder surface. This is :

$$dW_{in} = \int_{Si} (P - P_0) d_{li} \bullet d_{Si} = (P - P_0) \int_{Si} d_{li} \bullet d_{Si} = P' dV \qquad (1)$$

where P is the absolute internal gas pressure, P_0 the environment pressure (1 atm = 1.0336 bar), P' the relative pressure, S_i the total inner surface, d_{Si} the area vector, d_{li} the inner surface displacement, and dV the volume change.

The output work W_{out} is done when the actuator shortens in connection to the volume change, which is :

$$dW_{out} = -FdL \qquad (2)$$

where F is the axial tension, and dL the axial displacement. From the view of energy conservation, the input work should equal the output work if a system is to be without loss and energy storage. Assume the actuator is in the ideal condition thus :

$$dW_{out} = dW_{in} \qquad (3)$$

By replacing with equation (1) and equation (2) then $P'dV = -FdL$

$$\text{or } F = -P' \frac{dV}{dL} \qquad (4)$$

To estimate $\frac{dV}{dL}$, first we assume that the extensibility of the shell threads is very low, so that the actuator volume will only depend on its length. In addition, the middle portion of the actuator is modelled as a perfect cylinder with zero-wall-thickness, where L is the length of the cylinder, θ the angle between a braided thread and the cylinder long axis, D the diameter of the cylinder, n the number of turns of a thread, and b the thread length. L and D can be expressed as functions of θ with constant parameters n and b :

$$L = b \bullet \cos\theta \tag{5}$$

$$D = \frac{b \bullet \sin\theta}{n \bullet \pi} \tag{6}$$

The volume of the cylinder is then

$$V = \frac{1}{4}\pi \bullet D^2 L = \frac{b^3}{4\pi \bullet n^2}\sin^2\theta\cos\theta \tag{7}$$

From equation (4), F can be expressed as a function of P and θ :

$$F = -P' \frac{\frac{dV}{d\theta}}{\frac{dL}{d\theta}} = \frac{P' b^2\left(\cos^2\theta - \sin^2\theta\right)}{4\pi \bullet n^2} = \frac{P' b^2\left(3\cos^2\theta - 1\right)}{4\pi \bullet n^2}$$

$$F = \frac{\pi \bullet D_0^2 P'}{4}\left(3\cos^2\theta - 1\right) \tag{8}$$

where $D_0 = \frac{b}{n\pi}$, is the diameter when $\theta = 90°$.

The tension is thus linearly proportional to the pressure, and is a monotonic function of the braid angle $(0° < \theta < 90°)$. The maximum shortening will be reached when $F = 0$, that is $\theta = 54.7°$, this theoretical results have been verified.

Proposed Hand Master Design Specification

Prototype 1 will have the following features:

i). Position control on all four fingers and thumb using a gloved strain gauge based input device desinged and constructed at Salford. The accuracy of this device is approximately 0.5°.

ii). Force reflection into the thumb, index and middle finger, using one muscle per finger. This will be expanded as experience gained with this prototype.

iii). Maximum finger flexion > 90°

iv). Force per muscle system up to 50N at 6 bar.

v). Mass of single muscle 20g.

vi). Total mass of gloved system < 150g including glove.

vii). Force control better than 0.5N.

viii). Muscle response period < 100ms.

ix). Frequency response >2Hz.

x). Muscle mounted on dorsal surface of the hand.

Conclusions

At this stage of the project the initial design studies have been undertaken as suggested in the original proposal. All aspects of this activity have been satisfactorily concluded and the work is progressing to the next stage in line with the project plan outline. At this stage I do not foresee any reasons why this cannot be completed in a time and manner outlined in the proposal.

REFERENCES

[1]- I.A. Kapandji, "The physiology of the joints", Volume one, Churchill Livingstone, New York, 1982

[2]- P. M. Galley and A. L. Forster, " Human movement an introductory text for physiotherapy students", second edition, Churchill Livingstone, New York 1987.

[3]- "Joint motion method of measuring and recording", published by the American Academy of Orthopaedic Surgeons, 1965

[4]- M. Brattström, "Joint protection and rehabilitation in chronic rheumatic disorders", Wolfe Medical Publications Ltd, 1987

[5]- G. C. Burdea, "Force and touch feedback for virtual reality", John Wiley & Sons Inc, New York, 1997.

[6]- G. C. Burdea and P. Coiffet, "Virtual reality technology", John Wiley & Sons Inc, New York, 1994.

[7]- Virtual technologies Inc, Press release , "Virtual technologies Inc Introduces the CyberGrasp system", Palo Alto, August 20, 1997

[8]- Internet site http://www.virtex.com

[9]- C. P. Chou and B. Hannaford, "Measurement and modelling of the Mc Kibben pneumatic artificial muscles", IEEE Trancs on Robotics and Automation, volume 12 n 1, pages 90-102, 1996

[10]- C. P. Chou and B. Hannaford, "Static and dynamic characteristic of the Mc Kibben pneumatic artificial muscles", Procs IEEE International Conference on Robotics and Automation, San Diego, CA, may 1994

Hand Force Reflection using Pneumatic Muscle Actuators

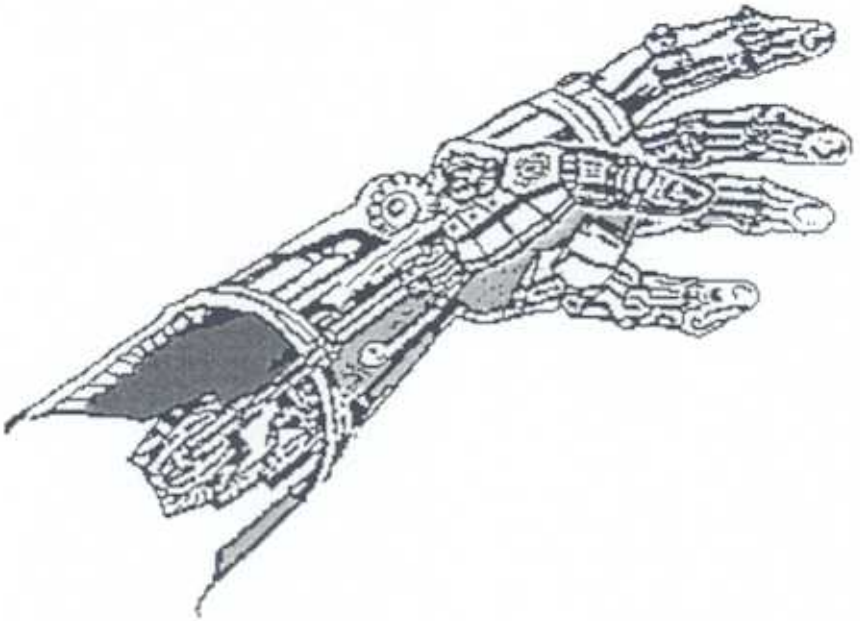

Quarterly Report - No.2

Contract F61708-98-W00134

Date 2-7-98

Report prepared by

C. Favede

Dept. of Electronic Eng.
University of Salford
Manchester, M5 4WT, UK

CONTENTS

INTRODUCTION

The aim of this project is the development of a hand force reflection device using pneumatic muscle actuators. The system characteristics will be dependent on the low mass of these actuators ands their very high power to weight ratio.

During the first three months of this project an extensive study of the background technology was undertaken placing the requirements clearly in context with regard to the aims of this work. In addition this work provided baseline designs for the construction of the hand force reflection device, or hand exoskeleton as it has been termed.

During the second three months of the project the following progress has been made.

i). The physical structure of the hand master exoskeleton.

ii). The control system components and layout.

iii).The input technique to measure the position of the finger/thumb joints.

These activities will be discussed in this report.

At this stage of the project, work is progressing in line with the plan outlined in the original proposal. Based on this progress, development towards the subsequent stages of the work will progress in line with expectations. At this stage there is no need to make any modifications to the work plan and presently it is expected that progress towards the completion of stage 3 will be made on time and to budget.

1- THE EXOSKELETON STRUCTURE

The primary objective of this research is the production of a hand master (or hand exoskeleton) which is capable of applying forces to the user's hand during the simulation of exploratory and manipulation tasks. To achieve this, a hand mounted system will be used which is required to monitor motion inputs from the fingers and thumb and constrain the motion outputs of the finger/thumb when in contact with a virtual object. As the hand master is to be portable it will be grounded on the user's hand, with the entire weight supported remote from the body. This may easily lead to user fatigue if the interface is too heavy and it is clear that a key feature in the development of these portable devices is the mass of the unit, both in the systems mechanical structure and in particular in the mass of the actuators.

The essential mechanical design requirements are therefore that the hand exoskeleton needs to be light, reducing or eliminating fatigue, while at the same instant being rigid enough that it cannot be bent when the pneumatic muscle actuators are energised.

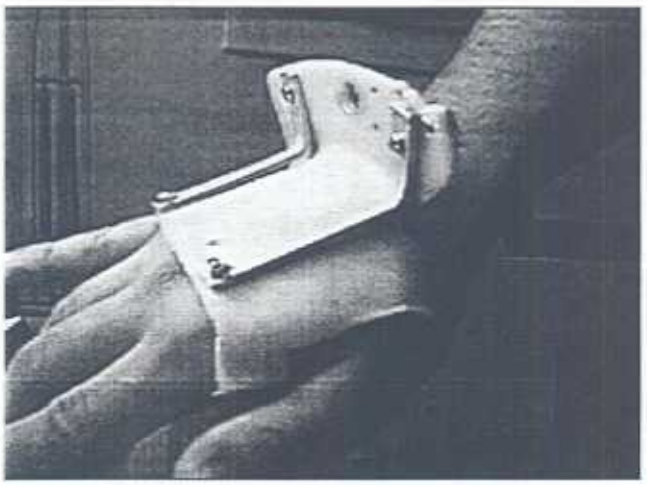

Fig. 1-1. The plastic structure.

From these comments an exoskeleton structure has been designed consisting of a rigid moulded plastic plate mounted on the back of the user's hand and bent to an angle of

90° at the wrist. This curved base is a necessary requirement to permit full flexion of the wrist and provide full unrestricted motion. The muscle actuators are attached between this plate and the phalangeal joints, and will be considered later.

The selection of the base material was an important aspect of the system design.. The plastic used in the construction is thermo deformable and can be easily moulded to suit the exact shape profile for the back of the operator's hand. This would clearly have been very difficult with aluminium or aluminium alloys. The main drawback of this structure is that the plastic in the selected thickness (3 mm) is not sufficiently rigid when the muscles are actuated. As a result the vertical portion of the support plate tends to bend at the wrist level. To overcome this deformation two aluminium brackets have been mounted on the plate to make the structure more stable, Figure 1-1. Although this does add some mass to the structure it is much less than with a conventional metal design.

This thermo-plastic support bracket is worn over the glove and secured in place with Velcro tape. This permits flexibility in the location of the mounts and adds comfort for the user. The glove used for the testing was a conventional leather with no special design modifications. This permits greater flexibility in the fitting. The pneumatic actuators controlling the motion of the constrained fingers are directly mounted on the vertical section of the base plate with the remote end of the actuator attached to the finger or thumb joint with the glove.

At the finger/thumb attachment point the actuator is connected to the distal section of the glove (end of the finger). Early tests with design showed that pulling directly of this glove section produced stretching of the leather which caused reductions in the motion control capacity and was also found to be very uncomfortable producing localised finger stress. To produce a more comfortable and controllable effect the thermoplastic was again used to form a finger 'thimble' moulded to the shape of the distal finger pad. This thimble, Figure 1-2, is attached to the pneumatic muscle actuator through a metal bracket shown at the top of Figure 1-2. This design was found to be much more comfortable and controllable.

Tests that this stage have concentrated for simplicity on the designs for the

middle finger an thumb. In these instances the actuators run from the attachment point at the wrist along the back of the hand to the finger/thumb. Thus when the muscles contract, a force is exerted at the user's fingertips.

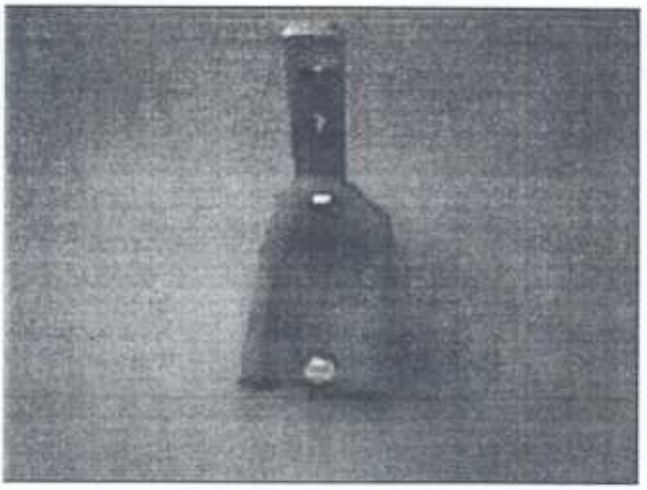

Fig. 1-2. The plastic thimble placed at the fingertip.

Early testing of this design philosophy revealed that in this simplistic form force could be exerted on the finger however, much of the force was along the axis of the finger rather than orthogonal to the joints. This tended to produce an unrealistic pulling sensation. In order to have the force exerted on the fingertip acting in the right direction, a metallic bracket was placed at the proximal interphalangeal joints of the user's fingers and at a height of three centimetres above the back of the user's hand, Figure 1-3. Thus the muscles are resting on the top of this bracket and therefore pull back the user's fingers in the required direction.

The thumb is positioned anterior to the palm and the other fingers, therefore its operation is not in the same direction as the other fingers and modifications to the above routing structure are needed to produce constrained sensation. After various tests, a solution was obtained which consists of grounding one end of the muscle to the end of the thumb with a plastic thimble, (as with the other fingers), and the other end of the muscle on the side of the hand (little finger side) and three centimetres below the palm. To do this a metallic plate perpendicular to the palm of the hand, and

going four centimetres below the palm is added to the structure, Figure 1-3. The muscle controlling the thumb motion is attached to this metallic plate running along the carpal bones of the wrist. In order to allow the muscle to be pulled the thumb in the correct direction a metallic cylinder perpendicular to the user's palm and placed at the thumb at the level of the metacarpo-carpal bones, has been added to the structure, Figure 1.3. These three aluminium sections and the thermo-plastic structure form the whole exoskeleton structure on which the muscles are grounded. This is illustrated in Figure 1-3.

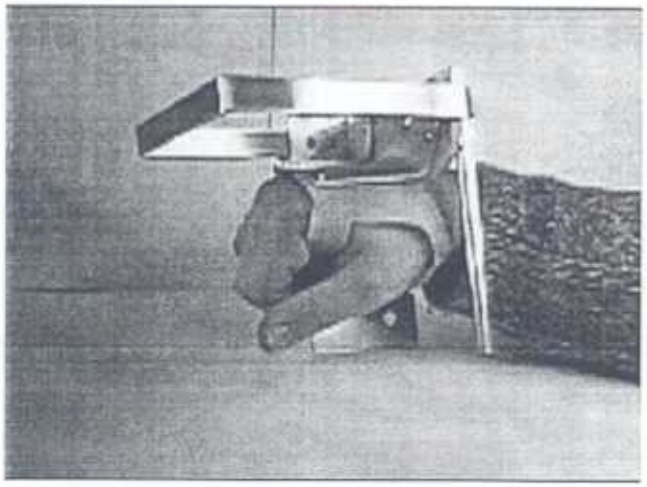

Fig. 1-3. The exoskeleton structure.

The final (and perhaps most important) feature of the hand exoskeleton is that it could be easy to wear. To achieve this the exoskeleton structure is attached to the back of a glove and the plastic thimbles are inserted inside each finger of the glove, Figure 1-4. This produces a device which is as easy to wear as putting a glove on a hand. At this stage the mechanism is effective but not aesthetically appealing. This is an aspect that will be considered at a future point in the project.

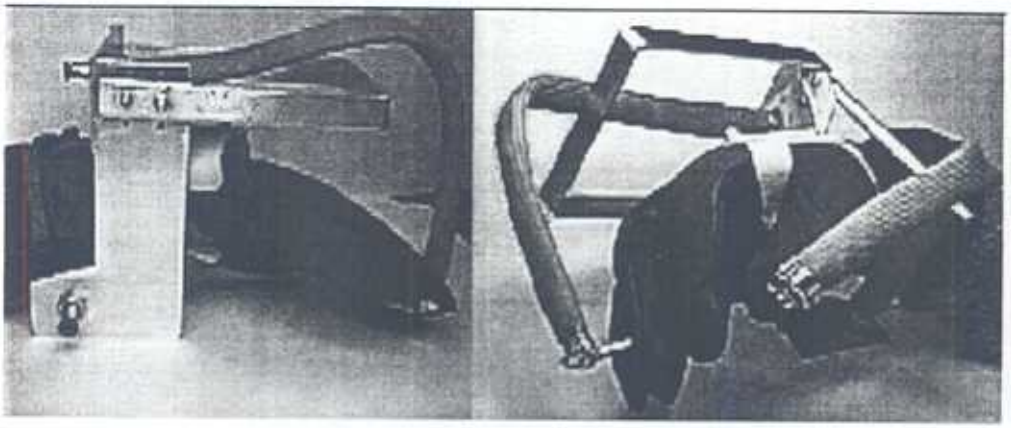

Fig. 1-4. The Hand master

This hand master allows full motion of the user's fingers, the muscles are mounted on the dorsal part of the hand, and overall weight of the hand master is less than 200g.

2- CONTROL OF THE PNEUMATIC MUSCLE ACTUATORS.

With the mechanical structure of the exoskeleton having been designed the next requirement was the mounting of the muscle actuators and in particular the control of the muscles. The overall schematic of the control system described in Figure 2-1.

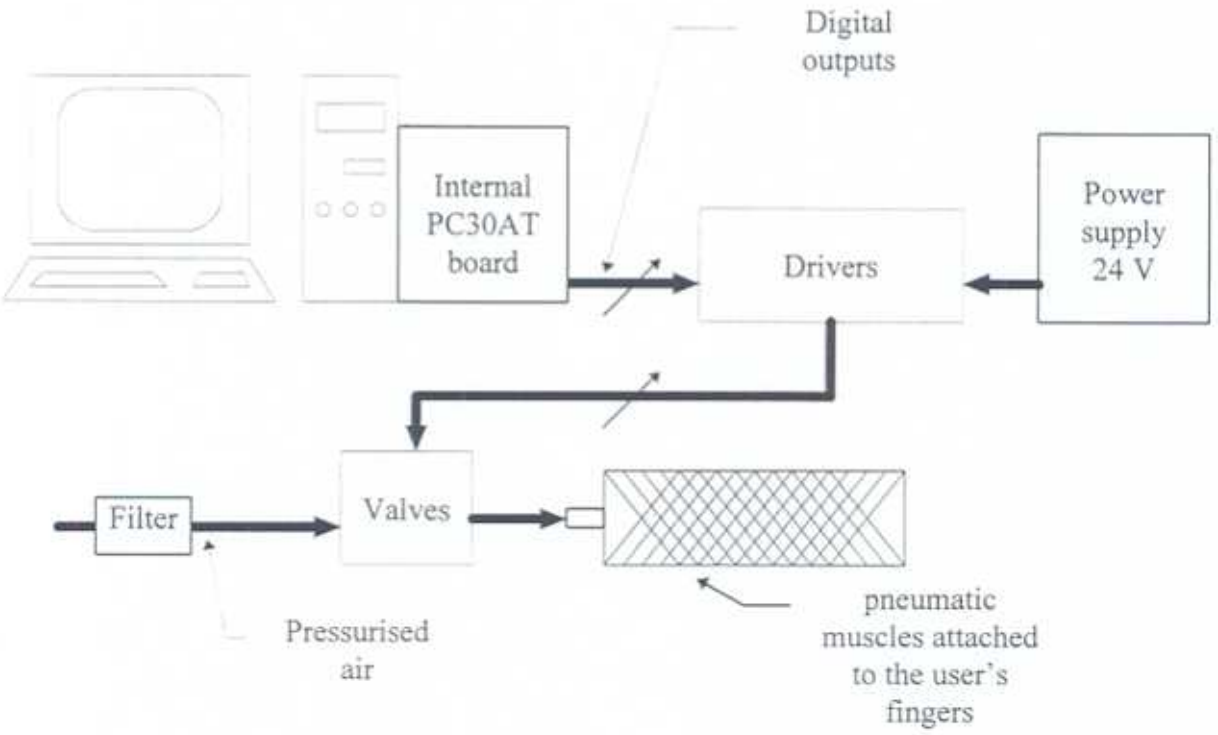

Fig. 2-1. Schematic representation of the system

The forces required for the system are generated by the motion of the pneumatic muscle actuators as they are contracted and relaxed when energised by an air supply operating at pressures of up to 500 kPa (5 bar - 60 psi).

The proposed control system design is considered below and can be studied in several sections

i). The muscle actuators described in the progress report 1. These muscles are 25 cm long with a diameter (when not energised) of 1 cm. In this format the muscles can

produce forces greater than 150N at the fingertip and provide displacement of up to 8 cm. This is more than adequate for the finger constraint requirements of this project.

ii). The control valves - these will be servo valves with pressure regulation and control using feedback on the finger displacement and forces induced at the joints.

iii). Control PC - The overall system is controlled by a PC. Thus data (control signals) will be sent from the PC to the other components of the system (valve driver boards) and the PC will receive input data on the condition of the system for feedback control. A multi function board will be used to design perform the A/D and D/A operations within the PC. This board will be a PC30 supplied by AMPLICOM LIVELINE LTD. The board was chosen because it has the required characteristics and has used for some time inside the robotic laboratory of the University providing a range of experience of the device.

The PC30 provides both analogue to digital (A/D) and digital to analogue (D/A) conversion facilities as well as parallel digital input/output and a timer/counter. The overall conversion time from analogue to digital is typically 35 μsec. The board has four D/A converters. Two of these are 12 bit and the other two are 8. Their output is either bipolar (-10V to +10V) or unipolar (0V to 10V). An on-board 8255 ppi provides three 8 bit input/output ports which can be interconnected in various ways to provide parallel TTL input or output, with or without handshake control.

iv). Valve Driver - Each valve uses a voltage of 1.2A varying between 0 - 24 V, whereas the output given by the digital output of the PC30 card is only between 0 and 5V and of only few mA. To solve this problem a drive circuit has been designed, Figure 2-2. The system will need one driver per valve, a board with four of these drivers has already been designed and tested satisfactorily.

This driver consists of two distinctive parts :

- The first part which includes the operational amplifier is an adaptation of a conventional impedance circuit and functioned as a buffer to protect the PC30 card.

- The second part, the bipolar transistor circuit provides the current needed for the valve's coil.

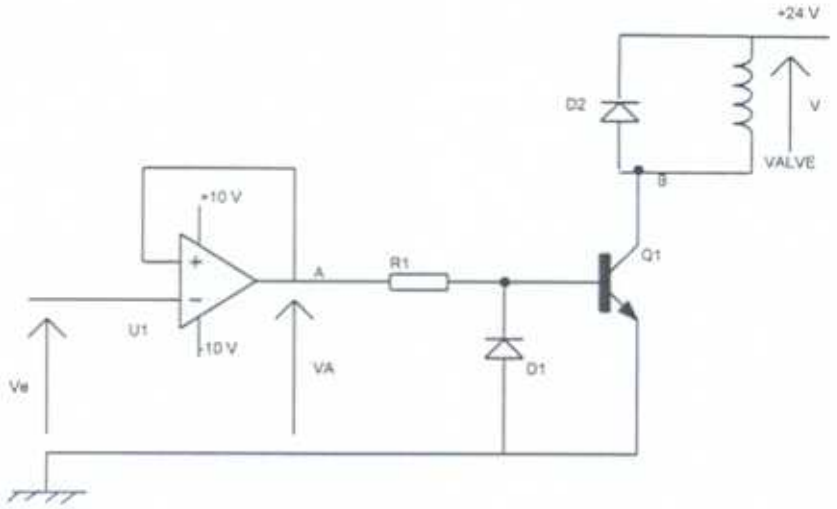

Fig. 2-2. Electrical power driver.

Component values :

R1 100 Ohms

D1 Diode 1N4001

D2 Diode 1N4001

Q1 bipolar transistor

U1 Operational amplifier

The behaviour of the overall circuit is illustrated in Figure 2-3.

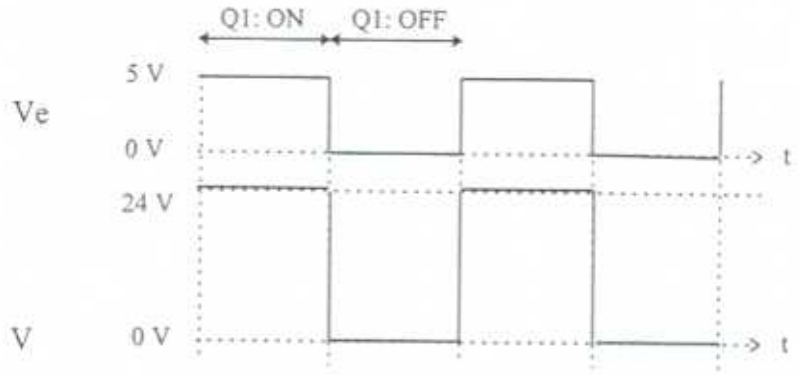

Fig. 2-3. Characteristics of the system.

When Ve = 5V, the transistor Q1 is not saturated, the current can go through the transistor Q1, the potential voltage in B (transistor collector) is 0. The input voltage of the valve is therefore 24V.

When Ve changes from 5V to 0, the transistor Q1 switches from the on-state to the off state and becomes saturated. The voltage in B is equal to the power voltage, 24V and the input voltage of the valve is therefore 0V.

A printed circuit board has been designed to control four valves.

3- THE INPUT DEVICE

A key feature of the exoskeleton force feedback system is the need to measure the position of the operator's fingers. To achieve this three approaches were tested.

The first of these was the use of Hall effect sensors. These sensors consist of two parts :

- a permanent magnet
- a current carrying conductor

The Hall effect occurs when a transverse magnetic field is applied to a current-carrying conductor. Due to the Lorentz force (F=-eVB), an electric field is created [1]. For the exoskeleton, the proposed design involved placing the current carrying conductor just in front of a finger joint and the permanent magnet (which creates a constant magnetic field) was attached just behind the finger joint. The magnetic field detected by the current carrying conductor will decrease, non-linearly, when the sensor is moving away (when the finger is bending). The sensor characteristic is shown in Figure 3-1.

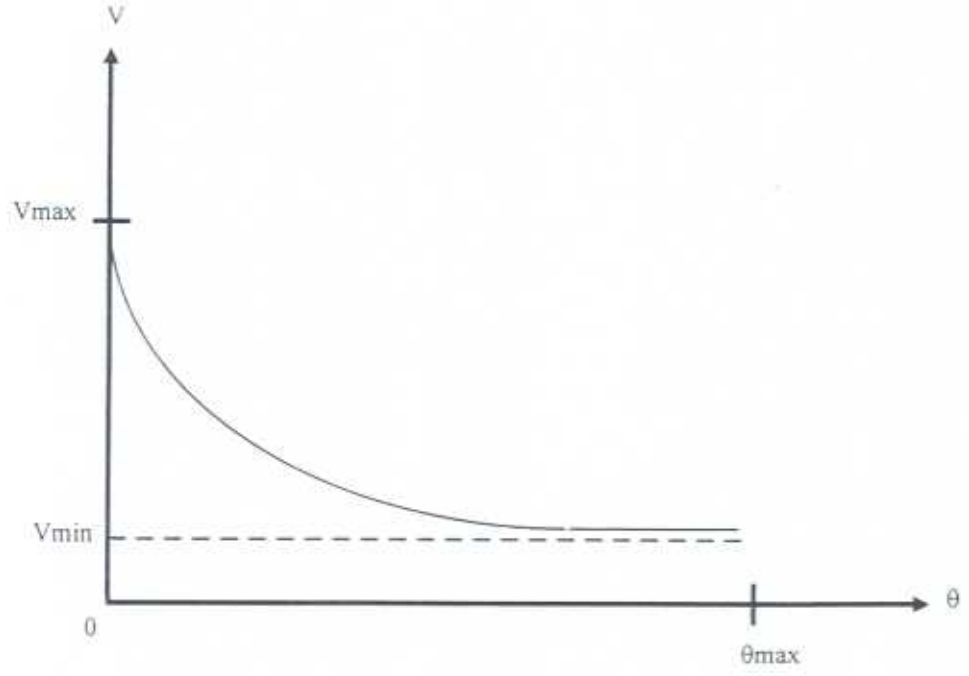

Fig.3-1. Hall effect sensor characteristic.

To operate effectively system calibration is required. This can be achieved but the complexity of the algorithm and the accuracy of the reading mean this solution is not optimal and was discontinued.

A second solution involved the use of a potentiometer attached to the side of the finger, a metallic probe is attached at shaft of the potentiometer with the other end located along the phalanx to be monitored. Thus when a finger is bending the shaft of the potentiometer rotates in proportion to the motion and the angle can be recorded. This solution gives good readings for the position of the finger, but was cumbersome due to the location of the potentiometer on the side of the hand and this resulted in a constrained finger motion.

The third approach tested was the use of strain gauges to measure the finger position. Strain gauges are resistive tranducers, wherein resistance varies as a consequence of strain changes within the gauge. By making this device part of a circuit, it is possible to produce an electric signal, that can, after suitable amplification monitor the finger position. Ideally a linear relationship between the final signal obtained and the original strain variation is necessary, so that the former can directly calibrated in the physical units of the latter. The strain gauge resistance is expressed in the form of $R+\Delta R$, where R is the resistance of the strain in absence of the strain (reference value) and ΔR represents the deviation from this reference value as a consequence of a change in the strain [2].

To measure resistance deviation, a method to convert ΔR to the voltage variation ΔV is to make the strain gauge part of a strain gauge bridge as illustrated in Figure 3-2.

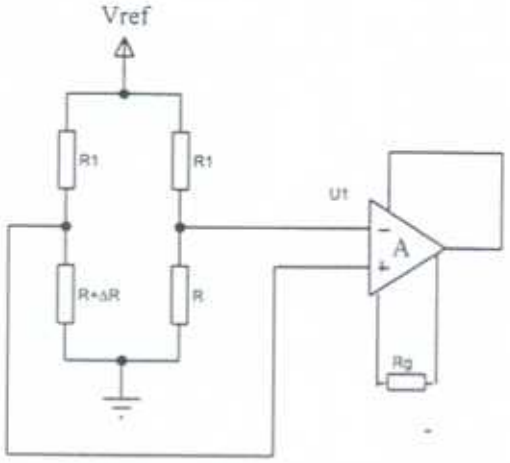

Fig. 3-2. A strain gauge bridge.

The strain gauge resistance changes when the device is lengthened or shortened :

$$\Delta R = 2R\frac{\Delta l}{l}$$

where R is the unstrained resistance and $\frac{\Delta l}{l}$ is the fractional elongation experienced by the gauge.

The deviation ΔR is extremely small in comparison to R, thus requiring a fairly high gain amplification to achieve a reasonable sensitivity. Furthermore precautions must be taken to prevent temperature variations from overshadowing the variations induced by strain.

A solution is to use pairs of strain gauges so that the temperature variations of one gauge compensate for the temperature variations of the other, thus leaving the ratios between their reference values constant [2]. Also to avoid cancelling out the variation due to strain, one of the two gauges must be of the R+ΔR type and the other of R-ΔR type. An additional advantage of using strain gauges in pairs is a doubling in bridge sensitivity. In fact the two gauges are bound to opposite sides of a thin plastic beam which is glued to a finger joint. When the finger is bent, the beam is then put under strain, one of the gauges will be lengthened and its resistance will therefore increase. The other will be shortened and its resistance will decrease.

The circuit illustrated in Figure 3-3 has been designed for each joint.

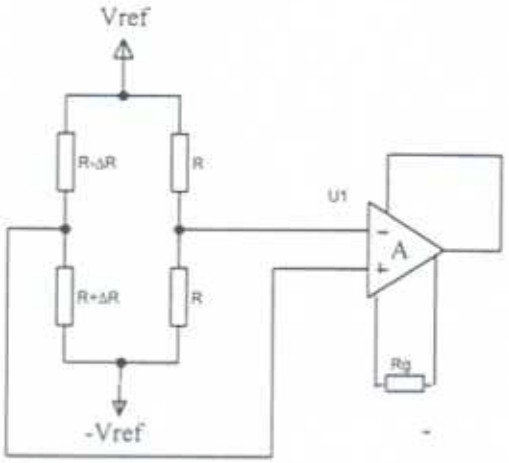

Fig. 3-3. The strain gauge circuit to measure the finger position.

To achieve the amplification stage, a INA114AP (Burr-Brown) operational amplifier has been used. This operational amplifier is a general purpose operational amplifier offering excellent accuracy. The gain of this operational amplifier can be set from 1 to 10000 with only a single resistor.

Gain for this system is given as : $G = 1 + \frac{50k\Omega}{R_G}$ [3].

This circuit converts the finger position into a voltage which is then sent to the computer via the PC30 board. The latter uses its A/D function to display the position of the finger on the computer screen. The tests the resolution of this input glove was found to be better than 0.3°. A glove instrumented with strain gauges is illustrated in Figure 3-4. To make the use of the exoskeleton simple the strain gauges will be instrumented directly on the hand master which means that there will be a need for only one instrument/force reflection glove.

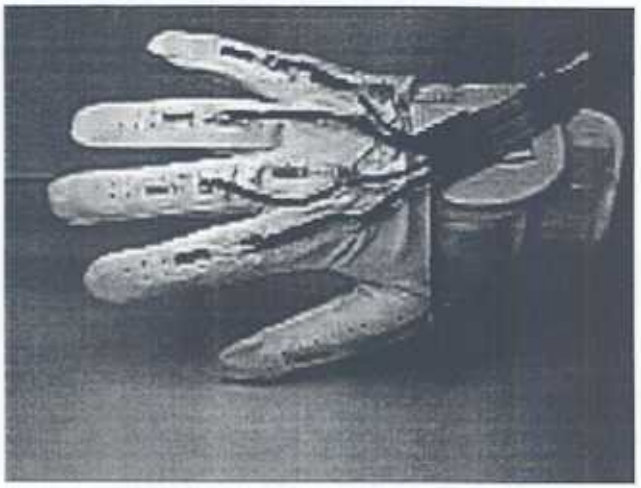

Fig. 3-4. The glove instrumented with strain gauges.

CONCLUSION

At this stage of the project, a light actuated exoskeleton has been designed. At present, this exoskeleton is actuated by two muscles and exhibits the characteristics mentioned in original proposal namely;

Low mass (<200g),

High force at the finger tips (>15N) and

full unecumbered motion of the user's fingers.

In addition an finger position detecting glove, instrumented using strain gauges has been designed. A number of techniques were appraised for this application including Hall effect sensors and miniature potentiometers but the strain gauge method was selected due to its compact nature which allows full motion of the user fingers while at the same time providing positional resolution of better than 0.3°.

Work has also been undertaken on the control of the system. This has involved a conceptual appraisal of the hardware and control systems to be used in the work. Drivers to control the valves which regulate the pressure within the muscles have been designed and constructed. Algorithms for control of the pneumatic actuators

have been studied. The development of a controlled hand exoskeleton will form the next stage of the project.

At present no additional time or change of the characteristics of the device is needed.

REFERENCES

[1] - C.S. Rangan, G.R.Sarma, V.S.V.Mani, "Instrumantation devices and systems", New Delhi, London : Tata Mc Graw-Hill,1983

[2] - "Design with operational amplifier and analog integrated circuit.", Sergio Franco, Mc Graw - Hill international editions, 1988.

[3] - INA114 data sheets, Burr-Brown corporation, 1992.

Hand Force Reflection using Pneumatic Muscle Actuators

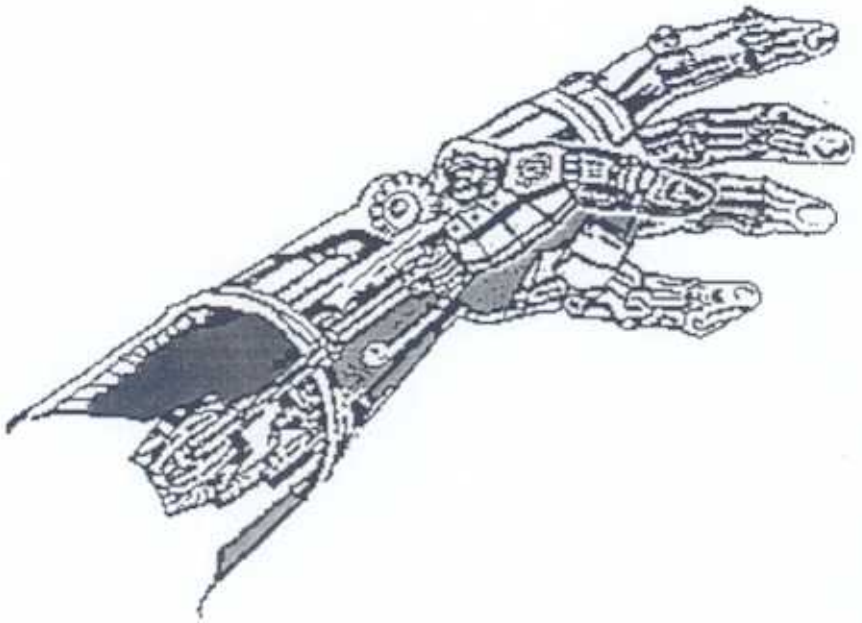

Quarterly Report – No.3

Contract F61708-98-W00134

Date 12-10-98

C. Favede and D.G.Caldwell
University of Salford
Manchester, M5 4WT
UK

CONTENTS

INTRODUCTION

The aim of this project is the development of a hand force reflecting device using pneumatic Muscle Actuators (pMAs).

During the first three months of this project a study of the background technology was undertaken in order to determine clearly the requirements of the system. During the second three months, a prototype showing the physical structure of the hand master was produced. This prototype is actuated by two muscles, one for the thumb and one for the fore finger and exhibits the following characteristics :

- low mass (< 200g)
- high force at the finger tips (>15 N)
- Full unencumbered motion of the user's fingers
- Monitoring of the finger position using a strain gauges instrumented glove.

During the third period of the project, month six to eight, control of the exoskeleton has been explored. This activity involved aspects of system position and force control. Motion was regulated by air flow and pressure regulation using a pulsed control strategy.

Using this system, the position of each finger can be accurately regulated. Control of the valves involves the use of a PC with dedicated data acquisition and analogue output boards. This monitor positions and regulates the pulsing and pressure within the actuators. As safety is vital in any device to be worn by a human, the computer will continuously monitor all force output to the system. All aspects of this control activity will be considered in this report.

At this stage of the project, work is progressing according to the plan outlined in the original proposal. There is no need to make any modifications to the work plan and it is expected that progress towards the completion of stage four will be made on time and to budget.

1- CONTROL OF THE HAND MASTER

1.1- Introduction

The aim of the project is to build a hand exoskeleton (or hand master) which is capable of applying forces to the user's hand during the virtual simulation of manipulation tasks.

This is achieved by controlling the finger position using pneumatic Muscle Actuators (pMAs). The pMAs are actuated using JOCOMATIC series 602 proportional 3 port solenoid valves. Pulse width modulation is used to drive these solenoid valves. Regulation of the airflow is achieved by varying the duty cycle of the pulse modulator, and hence the amount by which the muscles contract can be controlled. The hardware schematic of the control system is shown in Figure 1-1.

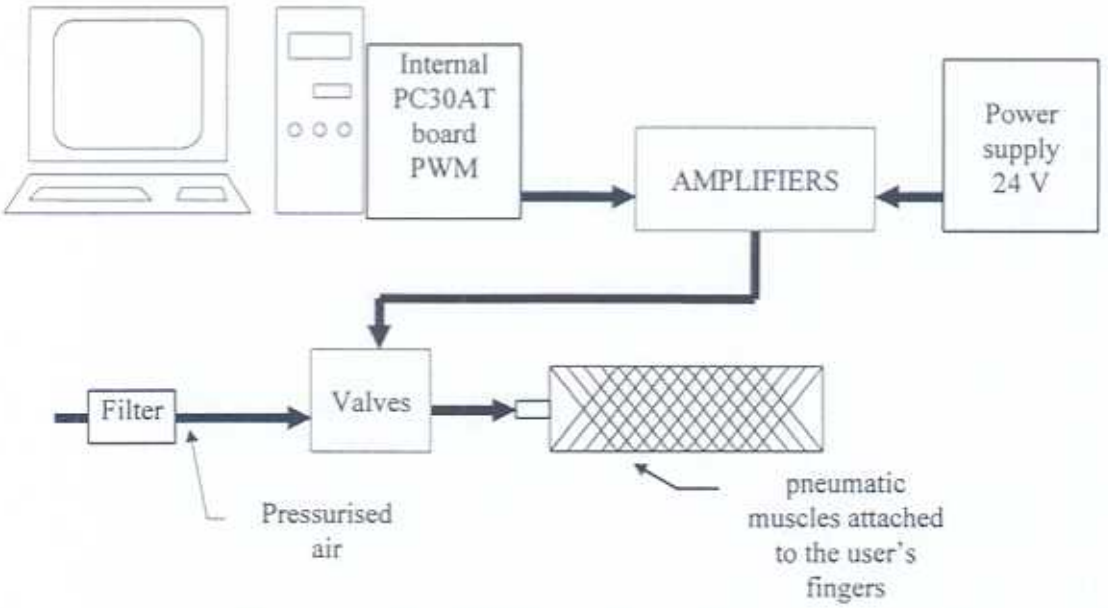

Fig. 1-1. Hardware control of the finger position.

Initially an open loop system, Figure 1-2 was tested but it is clear that this cannot fulfil the base specifications since disturbance inputs cannot be predicted or corrected.

Fig. 1-2. Open loop system

To compensate for disturbance inputs to the muscle contraction, finger position θ, or the finger force F closed loop control is necessary, Figure 1-3 [1].

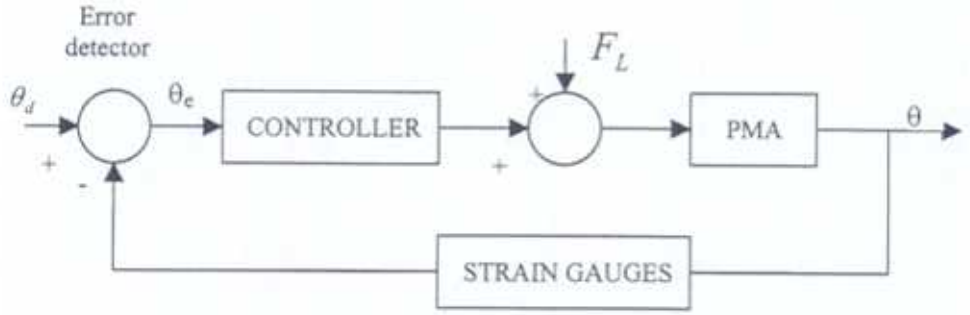

Fig. 1-3. Block diagram of the close loop exoskeleton control system

Figure 1-4 illustrates the different parameters of the system. The reference input θ_d sets the desired finger position (angle of the finger when the virtual object is grasped). The actual finger position θ should agree with the reference input and any error such as the load force F_L applied by the user's finger, which creates a change in the finger position, is sensed by the strain gauges sensors and the error detector. When a virtual object is grasped, the pMAs are actuated thus producing a force F at the fingertip, constraining the motion of the finger and simulating the presence of an object in the user hand. The user's fingers apply a force F_L directly oppose of this force F in order to grasp the object. This simulates the grip force and can be increased or decreased while maintaining a stable grasp or accurately manipulating the object.

At this stage only position control is possible as there is not direct sensing of F_L.

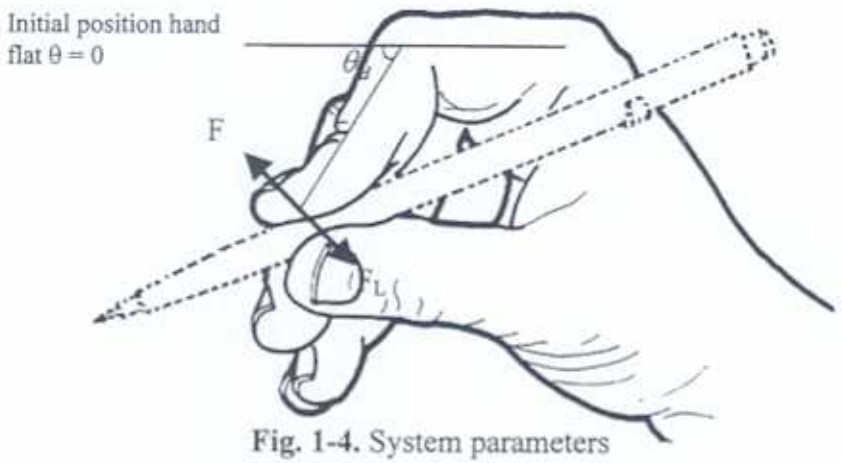

Fig. 1-4. System parameters

To control the simulating grasp position, the controller will operate on the error θ_e between the input and the present point and provide a signal to adjust the pressure in the pMA to correct the difference. In Figure 1-5(a), the finger position of the open loop system drops and settles at a lower value after a load force F_L is applied. Since the muscle internal pressure remains unchanged because there is no feedback, no correction is made. In Figure 1-5(b), the finger position of the close loop system is shown to recover quickly to the preset value after the application of the load force [2].

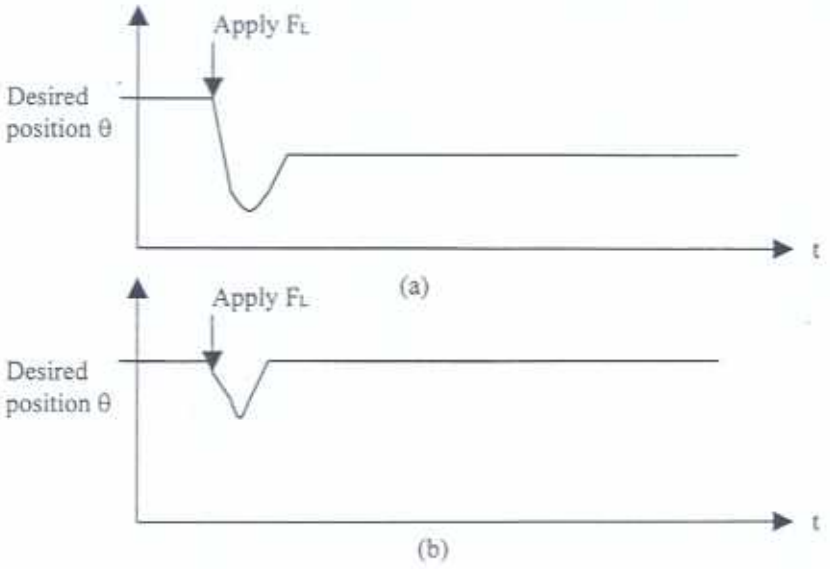

Fig. 1-5.(a) Typical response of the open loop system
(b) Typical response of the close loop system

The controlled system uses a PC with a PC30 data acquisition board and amplifiers, clearly described in the previous report to drive the solenoid valves. This system is therefore suited to digital control.

The principal advantage of the digital control is its flexibility. It is very easy to change the parameters of the controller, or implement another control loop by simply changing the software. Whereas analogue hardware systems requires rewiring, which is extremely time consuming and costly. A block diagram of a single loop digital control system is shown in Figure 1-6 [3].

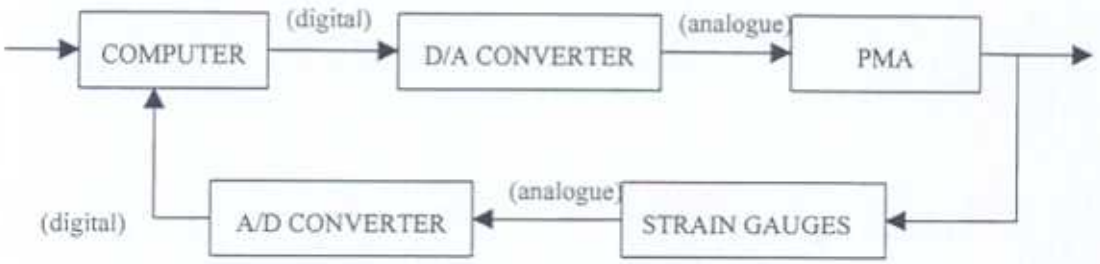

Fig. 1-6. Block diagram of the digital PMA control

The computer is programmed to provide an output so that the performance of the process is near or equal to the desired performance. A digital control system uses digital signals and a digital computer to control the process. The measurement data are converted from analogue to digital form, using the analogue to digital converter of the PC30 board. After processing the inputs, the computer provides an output in digital form. This output is then converted to analogue form by using the digital to analogue facilities of the PC30.

The computer uses data sampled at specified intervals, resulting in a time series of signals. These time series, called sampled data, can be transformed to the s-domain and ultimately, to the z-domain by the relation $z = e^{sT}$. The complex frequency domain in terms of z has properties similar to those of the Laplace s-domain.

In general the z-transform of a function $f(t)$ is defined as [4]:

$$Z\{f(t)\} = F(z) = \sum_{k=0}^{\infty} f(kT) z^{-k}$$

1.2- The PID controller

The output of a PID controller $y(t)$ comprises three components [5].

$$y(t) = K_1 \cdot e(t) + K_2 \cdot \int e(t)dt + K_3 \frac{de(t)}{dt}$$

where $e(t) = r(t) - c(t)$ = error (deviation)

$r(t)$ = reference input (setpoint)

$c(t)$ = controlled output

More commonly, $y(t)$ is written as

$$y(t) = K \cdot \left(1 + \frac{1}{T_i} \int e(t)dt + T_d \frac{de(t)}{dt}\right)$$

Where K = proportional gain

T_i = integral action time (constant)

T_d = derivative action time (constant)

Thus $y(t)$ comprises three terms a proportional term, an integral term, and a derivative term, which gives rise to the name "Proportional + Integral + Derivative" (PID) controller.

The proportional term is almost always used. The purpose of the integral term is to eliminate the steady state errors (offsets) in the control loop without significantly affecting dynamic performance. The purpose of the derivative term is to improve the dynamic performance, faster response and less overshoot. The proportional term is

always used in conjunction with the derivative term. The combinations of terms normally used are : proportional alone, integral alone (rarely), proportional plus integral (PI controller), proportional plus derivative (PD controller), and proportional plus integral plus derivative (PID controller).

The transfer function of the controller in the Laplace domain is, ideally [4]:

$$G(s)=\frac{Y(s)}{E(s)}=K\left(1+\frac{1}{sT_i}+sT_d\right)$$

This has been implemented in analogue controllers (electronic and pneumatic) for many years but in this case it will be digitally implemented

The transfer function can be discretised using numerical integration. There are several approaches possible for numerical integration [5], including :

i) Forward rule in this case $s=\frac{z-1}{T}$

ii) Backward rule where $s=\frac{z-1}{Tz}$

iii) Trapezoidal rule which lead to $s=\frac{2(z-1)}{T(z+1)}$

iv) Simpsons rule where $s=\frac{3(z^2-1)}{T(z^2+4z+1)}$

However for integration, the trapezoidal rule is preferred for accuracy reasons, while the backward rule is used for differenciation for simplicity reasons [5].

Thus the discrete transfer function becomes :

$$G(Z)=\frac{Y(Z)}{E(Z)}=K\left(1+\frac{T(z+1)}{2T_i(z-1)}+\frac{T_d(z-1)}{Tz}\right)$$

$$\Leftrightarrow Y(Z)=K\left(1+\frac{T(1+z^{-1})}{2T_i(1-z^{-1})}+\frac{T_d}{T}(1-z^{-1})\right)E(Z)$$

Where T is the sampling interval.

While this transfer function can be simplified and an overall difference equation

obtained, it is preferable for practical reasons to determine the component terms individually and then combine them to determine the output.

Initially, K is excluded and P is defined as the proportional term, D as the derivative term and I as the integral term.

(i) Proportional

$$P(Z) = E(Z)$$

$$P_n = e_n$$

(ii) Integral

$$I(Z) = \frac{T\left(1+z^{-1}\right)}{2T_i\left(1-z^{-1}\right)}E(Z)$$

$$\Leftrightarrow I(Z)\left(1-z^{-1}\right) = \frac{T}{2T_i}\left(1+z^{-1}\right)E(Z)$$

$$i_n - i_{n-1} = \frac{T}{2T_i}\left(e_n + e_{n-1}\right)$$

$$\Leftrightarrow i_n = \frac{T}{2T_i}\left(e_n + e_{n-1}\right) + i_{n-1}$$

(iii) Derivative

$$D(Z) = \frac{T_d}{T}\left(1-z^{-1}\right)E(Z)$$

$$d_n = \frac{T_d}{T}\left(e_n - e_{n-1}\right)$$

The output is then evaluated as $y_n = K\left(p_n + i_n + d_n\right)$

One problem encountered during the implementation of the controller was integral windup. When this occurs the integral term continues to change although the output device (valve) is in saturation. This causes a delay in output coming out of saturation, as shown in Figure 1-7 for an integrator followed by a saturation element and subject to a square wave input. The solution is to halt the integration process when the output

device is in saturation (valve open time greater than the period of the PWM) [6].

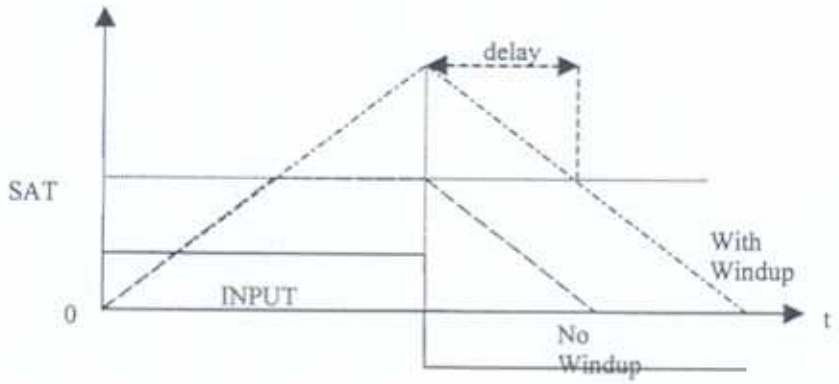

Fig. 1-7. The windup effect

2-TESTS AND RESULTS

As previously explained, the valves are controlled using PWM. By changing the duty cycle of the pulses the pressure inside the pMAs change and, this regulates their length. The period of the PWM signal has been set at 80Hz [6]. The system is controlled using a PC and a program in C language. The general flowchart of the software is given in Figure 2-1.

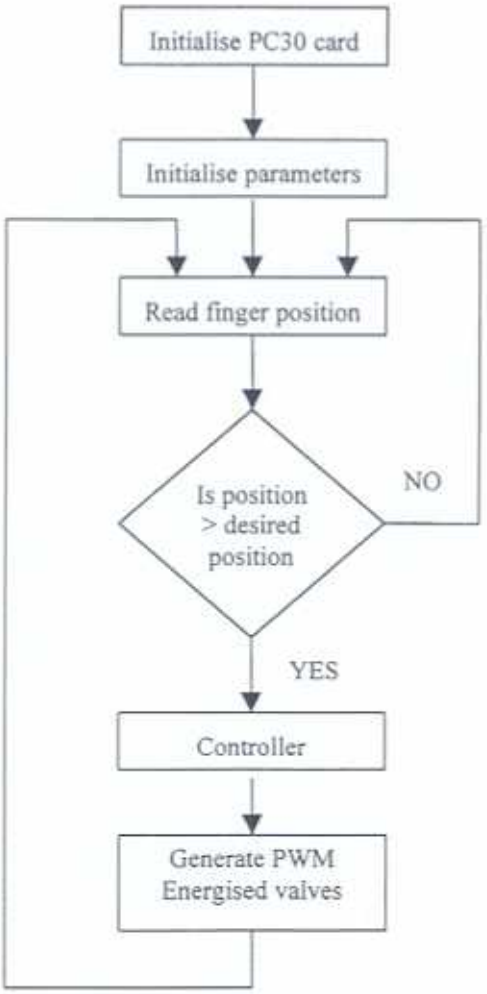

Fig 2.1- General flowchart of the computer program

i) The data acquisition card, the PC30 needs to be initialised in order to perform A/D and D/A conversion.

ii) Initialisation of parameters are set including the controller gains, channels selection of the card used and the desired finger position θ_d.

iii) The position of the finger θ is read by converting the analogue values returned by the strain gauges mounted on to the glove to digital values which can be used by the computer program (see previous report [7]).

iv) Finger positions θ are compared to the desired angles θ_d. If one of them is greater than the desired position, the controller calculates, according to the controller law, the time interval for which the valve should be open (the new value of the duty cycle) or else no corrective action is needed and the program goes to iii).

v) The muscles are actuated using the value calculated by the controller.

A proportional controller, proportional derivative controller, proportional integral controller, and proportional plus integral plus derivative controller have been implemented and tested using this computer algorithm.

2.1- The proportional controller

First the simplest proportional controller was implemented. The flowchart of this proportional controller is given in Figure 2-2.

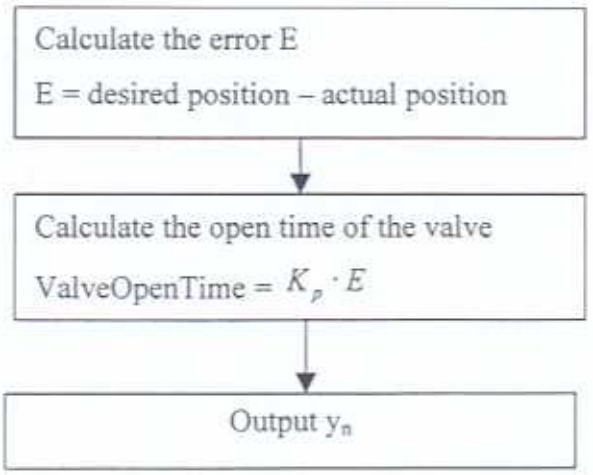

Fig. 2-2. Flowchart of the proportional controller

The first proportional controller implemented and tested with the system had a gain $K_p = 10$. Figure 2.3, shows the finger position for this controller when a virtual object is grasped by the user. The desired angle θ_d is set at 20°. This figure also shows the duty cycle of the PWM signal which is used to drive the solenoid valve.

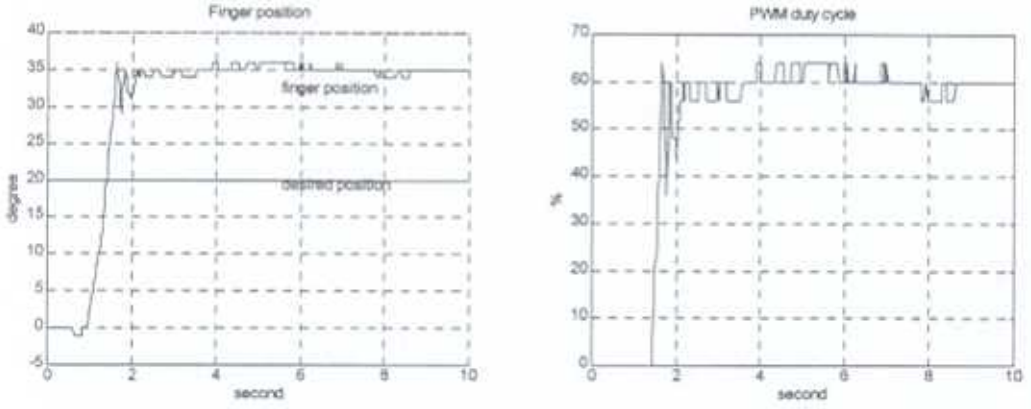

Fig. 2-3. Position of the finger for $K_p = 10$
Duty cycle of the PWM

In this case, with the proportional gain K_p set to 10, the output signal is far from the expected value. As can be seen on Figure 2-3, the finger position is stabilised at 35° but the desired position is $\theta_d = 20°$. The steady state error is then approximately 15° which is totally unacceptable. To obtain better result the proportional gain of the controller was increased.

With the gain $K_p = 20$, and the results obtained when a virtual object is grasped are shown in Figure 2-4 together with the duty cycle of the PWM signal which drive the valve.

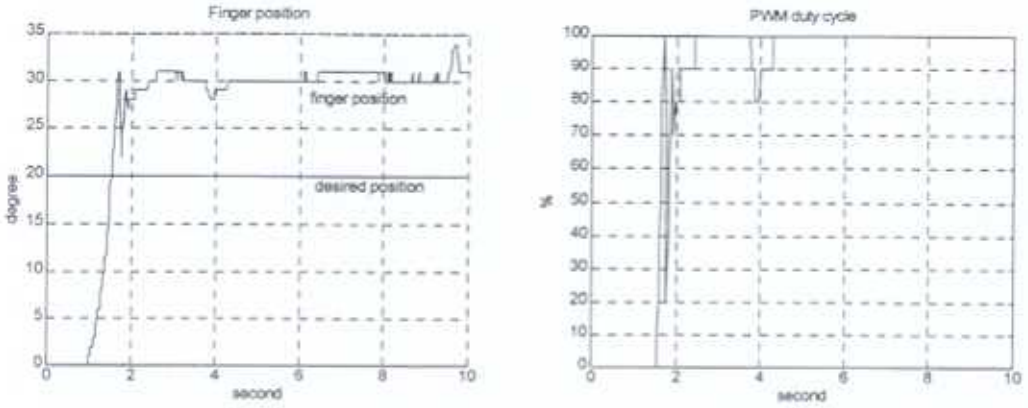

Fig. 2-4. Position of the finger for $K_p = 20$
Duty cycle of the PWM

As can be seen, the output signal is better than when $K_p = 10$, the steady state error is approximately 10°, however further improvement is desirable and a new series of tests were undertaken with $K_p = 50$.

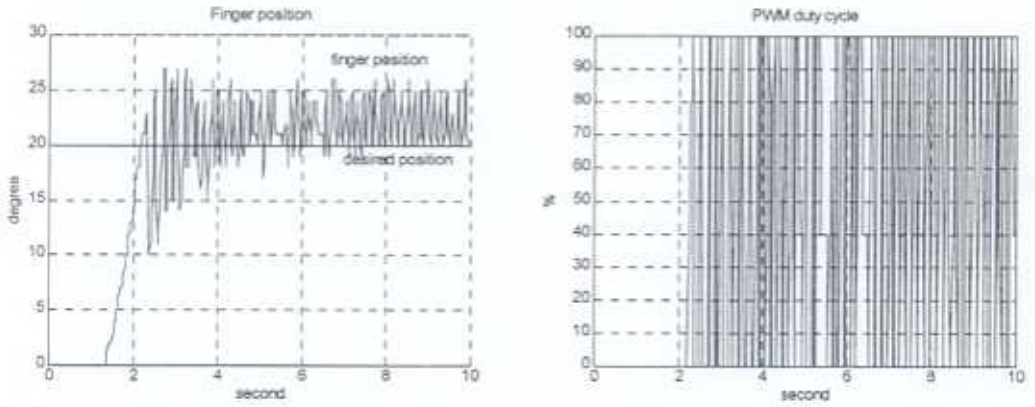

Fig. 2-5. Position of the finger for $K_p = 50$
Duty cycle of the PWM

By increasing the proportional gain, the finger position should improve and settle very close to the reference position (20°), but as seen in Figure 2-5, the system becomes unstable, because the proportional gain is too large. The PWM cycle illustrated in Figure 2-5 is always at 100% or 0% which means that the valve is fully open or fully closed but no intermittant position is available. Therefore the best results obtained with a proportional controller are when $K_p = 20$, and the steady state error is then 10°.

This result is not very good and another type of controller has to be tested to improve the performance of the system.

2.2- The proportional derivative controller

To improve the performances of the proportional controller, a proportional plus derivative (PD) controller has been developed. The flowchart of the PD controller is given in Figure 2-6.

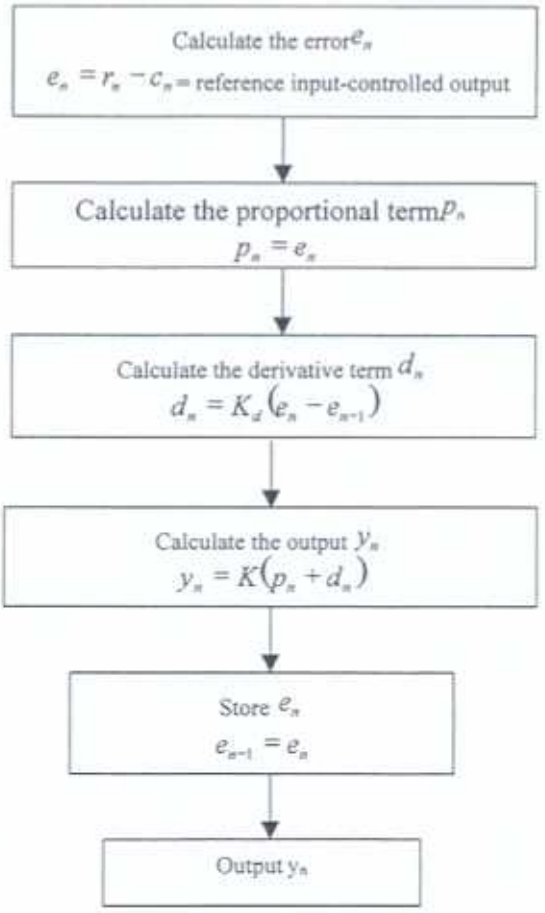

Fig. 2-6. Flowchart of the PD controller

The effect of the PD controller is similar to the introduction of a zero to the system transfer function [5]. It can be used to cancel a pole which deteriorates the dynamic behaviour of the system. It should improve the closed loop dynamic performance such

as faster response or a reduced overshoot, without detriment to the systems accuracy [1].

The first PD controller implemented and tested with the system had a proportional gain $K_p = 10$, and a derivative gain $K_d = 5$. Figure 2.7, shows the finger position for this controller when a virtual object is grasped by the user. This figure also shows the duty cycle of the PWM signal which is used to drive the solenoid valve.

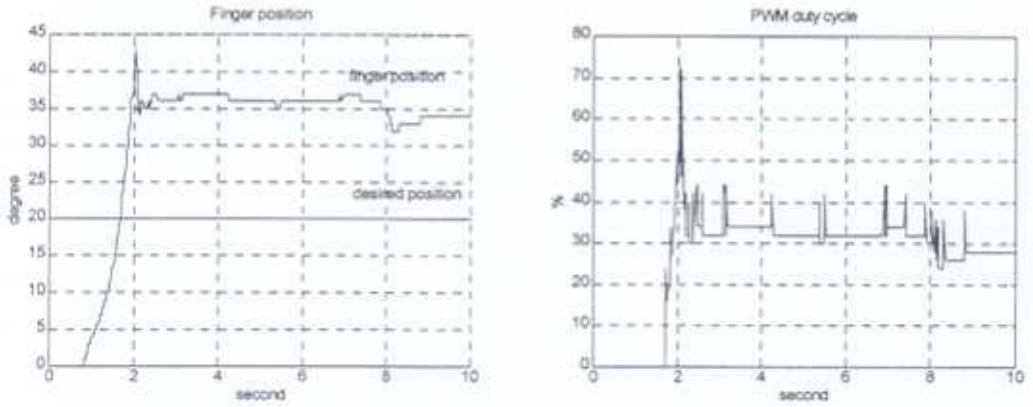

Fig. 2-7. Position of the finger for $K_p = 10$, $K_d = 5$
Duty cycle of the PWM

The output signal is settled around 35°, the steady state error is 15°. Direct comparison with the proportional controller of the same gain tested earlier cannot be done since the finger velocities or force grasping the virtual object may not be the same but it seen that the response of the system was faster and that the overshoot has been reduced.

Another series of tests has been undertaken with the derivative gain $K_d = 9$, and a proportional gain $K_p = 20$.

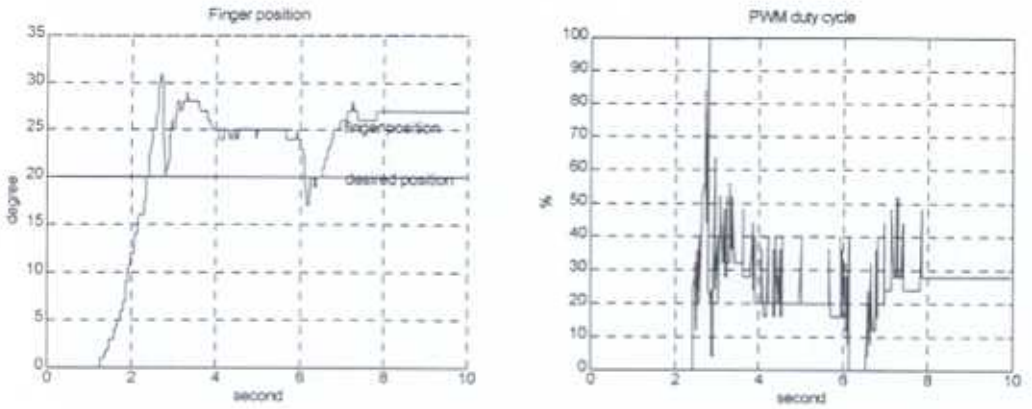

Fig. 2-8. Position of the finger for $K_p = 20$, $K_d = 9$
Duty cycle of the PWM

As expected, the behaviour of the system is better than the one obtain with the proportional controller of the same gain, Figure 2-8. The steady state error is approximately 7°, but must be reduced.

2.3- The proportional integral controller

In this design the output of the controller is the sum of two terms, the proportional term and the integral term. The output of the controller will continue to change as long as the error is not equal to zero. The effect of the integral action is to reduce the steady state error. The flowchart of the PI controller is given in Figure 2-9. As previously explained the algorithm also prevents integral windup.

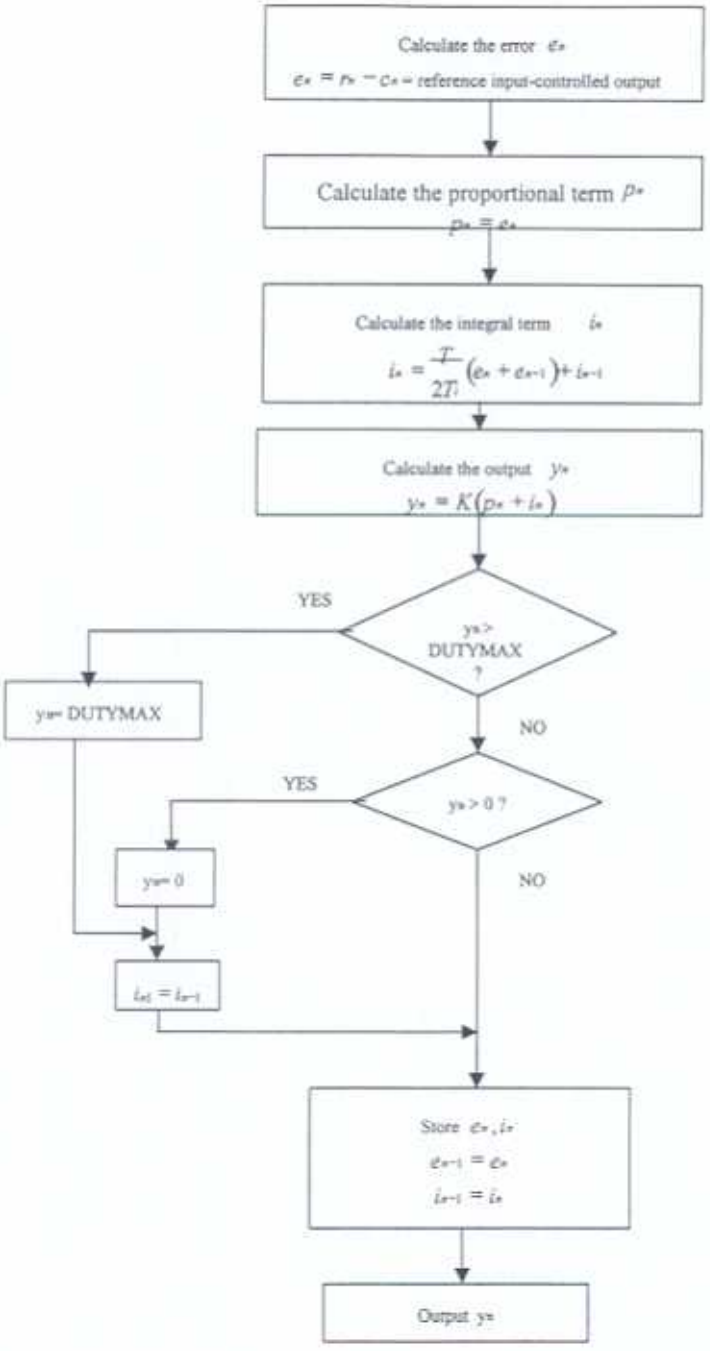

Fig. 2-9. Flowchart of the PI controller

The first PI controller tested had a proportional gain K_p of 10 and an integral gain K_i of 5. Figure 2-10, shows the finger position, and also the PWM duty cycle signal

which drives the valve.

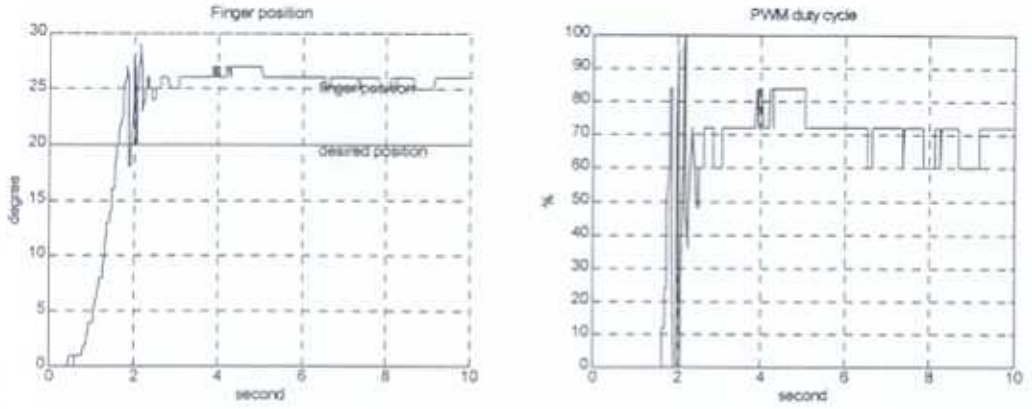

Fig. 2-10. Position of the finger for $K_p = 10,\ K_i = 5$
Duty cycle of the PWM

As shown in Figure 2-10, the output response is better than with a simple proportional controller but the steady state fails to reach 0° in the 10 seconds experiment, and it is still around 5°.

In order to reduce the steady state error another PI controller, with the same proportional gain as before but with its integral gain K_i increased to 9, was tested.

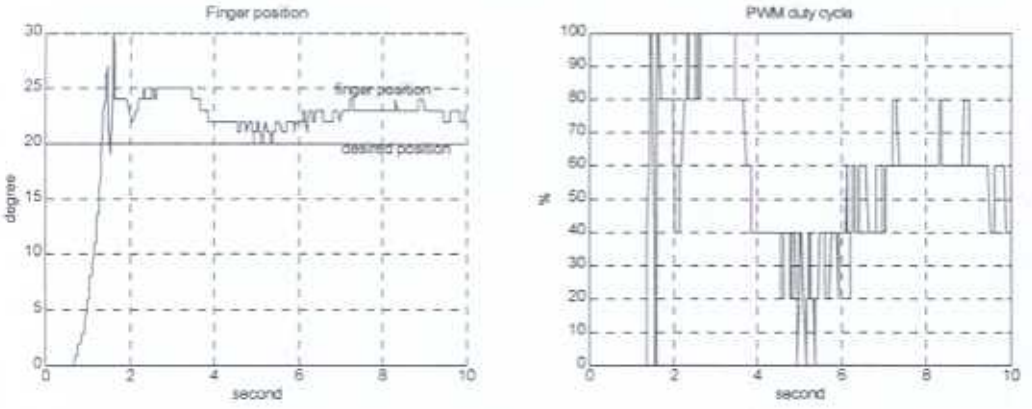

Fig. 2-11. Position of the finger for $K_p = 10,\ K_i = 9$
Duty cycle of the PWM

As seen in Figure 2-11, the steady state error has decreased and settled around 3°. The results obtained with the PI and PD controllers are better than those obtained for the proportional controller. However one option remained to be tested, to improve the performance of the system even more, the PID controller.

2.4- Proportional derivative integral controller

The PID controller combines the advantages of the three other controllers previously implemented and tested. Figure 2-12 illustrates the algorithm of the PID controller, as with the PI system anti windup has been incorporated.

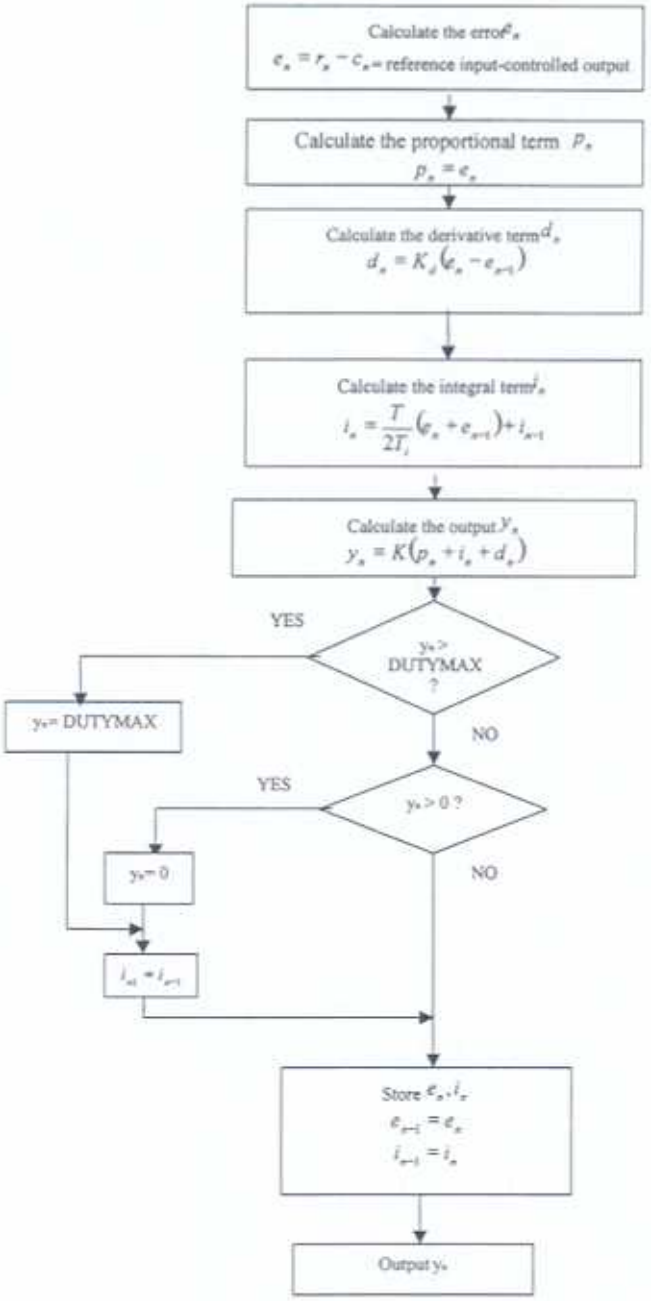

Fig. 2-12. Flowchart of the PID controller

The first PID controller tested had its proportional gain $K_p = 9$, its derivative gain $K_d = 3$, and its integral gain $K_i = 5$. Figure 2-13 shows the finger position when the virtual object is grasped, together with the PWM duty cycle signal which drives the solenoid valve.

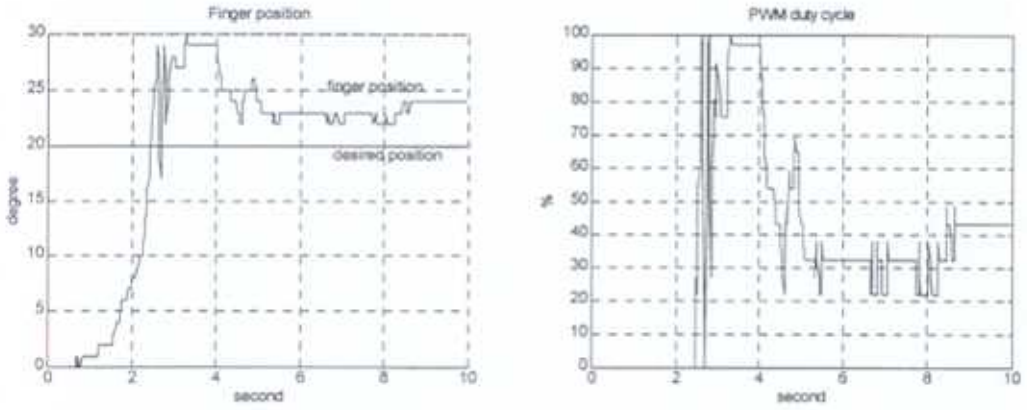

Fig. 2-13. Position of the finger for $K_p = 9$, $K_d = 3$, $K_i = 5$
Duty cycle of the PWM

At the end of the 10 seconds experiment the steady state error is still around 5°. To reduce the steady state error the integral gain was increased. The derivative gain was also increased in order to obtained a faster response and also decrease the overshoot. The second PID controller tested had a proportional gain $K_p = 9$, a derivative gain $K_d = 7$, and an integral gain $K_i = 7$. The finger position and the PWM duty cycle signal which drives the valve are illustrated in Figure 2-14.

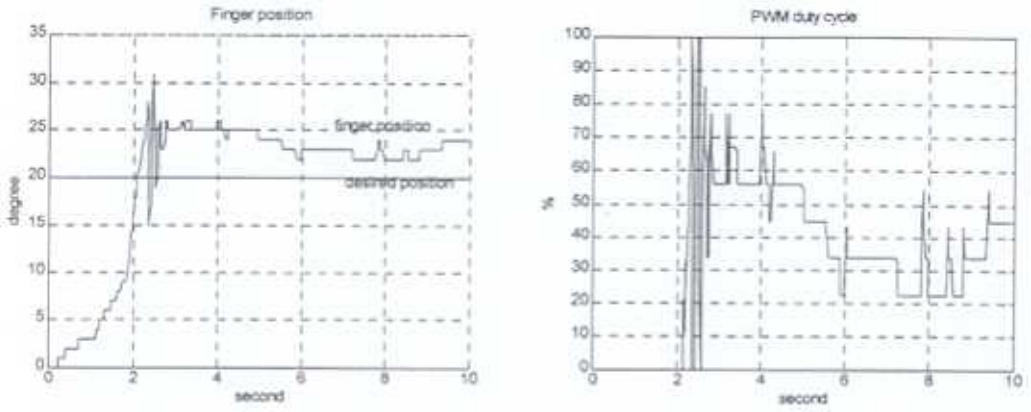

Fig. 2-14. Position of the finger for $K_p = 9$, $K_d = 7$, $K_i = 7$
Duty cycle of the PWM

The response obtained with this controller shows that at the end of the experiment the steady state error is down to 3°. The overshoot has also been reduced and the response is faster.

The final PID controller tested had a proportional gain $K_p = 14$, a derivative gain $K_d = 9$, and an integral gain $K_i = 9$, Figure 2-15 shows the results obtained.

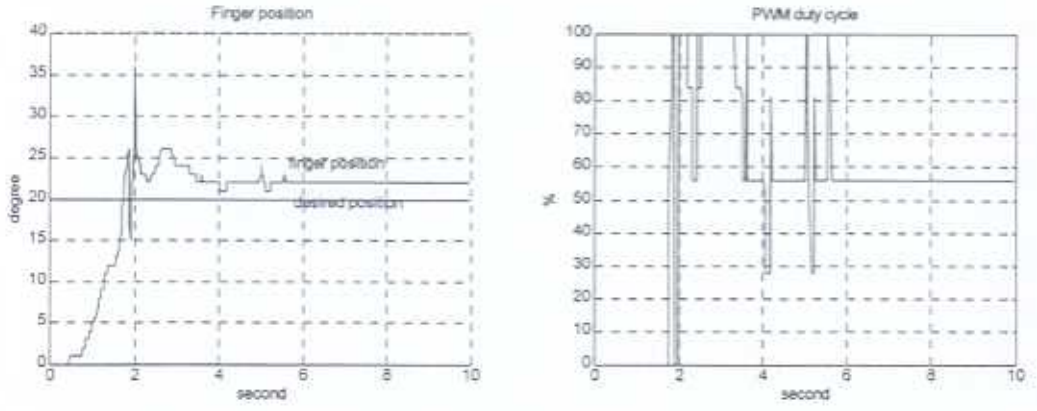

Fig. 2-15. Position of the finger for $K_p = 7$, $K_d = 7$, $K_i = 7$
Duty cycle of the PWM

The finger position is stable and the steady state error is around 1.5°.

CONCLUSION

At this stage of the project, a light actuated exoskeleton has been designed. At present this exoskeleton is actuated by two muscles [7] and provides a feedback force, greater than 15N at the fingertips. The system is instrumented by strain gauges in order to measure the finger positions. The system air supply is regulated using JOUCOMATIC proportional solenoid valves which are digitally controlled using a computer and a PID controller implemented in C. This controller allows accurate and fast control of the muscles providing realistic sensations when a virtual object is grasped.

The next stage of the project will add strain gauges to the exoskeleton in order to monitor the forces at the fingertips. A virtual reality demonstration program will also be developed.

At present, no additional time or change to the characteristics of the device is needed.

REFERENCES

[1]- B. C. Kuo, "Automatic control systems", seventh edition, Prentice Hall International editions, New Jersey, 1995.

[2]- P. H. Lewis and C. Yang, "Basic control systems engineering", Prentice Hall, New Jersey, 1997.

[3]- T. Dougherty, " Systems & Control, An introduction to linear, sampled & non-linear systems", World scientific publishing, Singapore, 1995.

[4]- K. Ogata, "Discrete-time control systems", second edition, Prentice Hall International editions, New Jersey, 1995.

[5]- R. C. Dorf and R. H. Bishop, "Modern control systems", seventh edition, Addison Wesley publishing company, 1995.

[6]- C. Favede and D. G. Caldwell, "Hand force reflection using pneumatic muscle actuators – Quarterly report No 1", Mars 98.

[7]- C. Favede and D. G. Caldwell, "Hand force reflection using pneumatic muscle actuators – Quarterly report No 2", July 98.